ISSN 2277-3061

Parametric Study of Silicon–Based Optical Leaky-Wave Antenna

Ali A. Hummadi, R. S. Fyath
M.Sc. Searcher, College of Engineering, Alnahrain University, Baghdad, Iraq
Professor, College of Engineering, Alnahrain University, Baghdad, Iraq

ABSTRACT

Parametric study is presented for 1550 nm CMOS compatible optical leaky wave antenna. The antenna is designed with Si_3N_4 waveguide perturbed periodically with silicon. The silicon perturbations are used to transform the guided mode into a leaky mode radiated to the surrounding space. Simulation results are obtained using the commercial software package CST STUDIO SUITE 2012 and indicate clearly the strong dependence of radiation parameters on the number and dimensions of the silicon perturbations.

Indexing terms/Keywords

Optical leaky wave antenna (OLWA); Silicon-based antenna; Silicon optical antenna.

Academic Discipline and Sub-Disciplines

Electronics and Data Communications.

SUBJECT CLASSIFICATION

Optical antennas.

TYPE (METHOD/APPROACH)

Simulation Work.

ISSN 2277-3061

1. INTRODUCTION

The past decade has witnessed a regain of interest in microwave leaky-wave antennas (LWA) due to the progress in material fabrication and the emergence of artificial materials [1,2]. They provide numerous advantages such as low complexity feeding network, high efficiency, and compatibility with established manufacturing techniques [3].LWAs are popular in the microwave band and above, because they can achieve high directivity with simple structure, without the need of complicated and costly feed network as typically used in a phase-array antenna [4].

There are two types of LWA, uniform [5] and periodic [6,7] whose operation principles can be summarized as follows [8]. The uniform antenna has uniform guided structure and can provide radiation into the forward quadrant. It can yield scanning from broad side to forward end fire directions. The periodic antenna has an array of periodic guided-wave structures and provides scanning range from backward end fire through broad side directions in to a part of forward quadrant. The dominant mode on the uniform and periodic antenna is fast wave and slow wave, respectively. The dominant mode on periodic LWAs does not radiate and radiation is achieved by using one of its space harmonics [9].

Recently, there is increasing interest to extend the concepts of microwave antennas to optical frequencies leading to optical antennas [10, 11]. These antennas have the ability to control the emission and scattering of light with a small-scale footprint [12]. Similar to microwave antennas, their purpose is to convert the energy of free propagating radiation to localized energy and vice versa [13].This leads to enhancement of the interaction between light and matter which is useful to boost the efficiency of optical sources and detectors [14,15].Different types of optical antennas have been proposed, analyzed, and fabricated. Among these types, the optical leaky-wave antenna (OLWA) (which uses the optical wave travelling on guide structure as the main radiating mechanism to the surrounding space) attracts increasing interest [16, 17]. This antenna is capable of producing high directivity narrow beams with steering (scanning) capability. These features make OLWAs useful for certain applications such as planar imaging [18], LIDAR [19], and Wireless optical interconnect [20].

Recently, a novel silicon-based OLWA has been proposed to provide very directive radiation at 1550 nm [21]. The structure is CMOS compatible and hence can be fabricated on silicon-on-insulator platform which is suitable for both optoelectronic and photonic integration [22].Further, the radiation parameters of the reported antenna can be controlled by introducing excess carriers in the silicon via electronic or optical injection [22,23].

The OLWA proposed in [21] consists of SiO_2-Si_3N_4-SiO_2 waveguide with silicon perturbations positioned on the bottom side of the silicon nitride core as shown in Fig.1. The radiation characteristics of this antenna have been investigated by the same research group and the results have been reported in a series of papers [21-23]. In [21], the propagation constant and attenuation coefficient of the leaky wave in the periodic structure have been extracted from full-wave simulations obtained using commercially software packages (COMSOL and HFSS). The results show that the far-field radiation patterns in silicon and air environments predicted by the leaky-wave theory agree well with the ones obtained by the full-wave simulations. Further, it has been shown that the use of semiconductor corrugations facilitate electronic tuning of the antenna carrier injection. In [22], the radiation pattern has been investigated further when the device is subjected to optical injection at visible wavelength (650 nm) to yield excess carrier generation in silicon. A new design based on integrating the OLWA with Fabry-Perot cavity has been proposed to overcome the limited control of the radiation intensity through excess carrier generation. The performance of this structure has been investigated further in [23] to address the control of radiation intensity in the broad-side direction via excess carrier generation in the semiconductor regions. The investigation has been extended further in [24] to characterize OLWA integrated in a ring resonator.

This paper investigates the effect of structure parameters on the far-field radiation of the OLWA proposed in [21]. Various radiation parameters are tracked during the parametric study such as scattering coefficients, radiation and total efficiencies, directivity, gain, main lobe magnitude and direction, side-lobe level, and angular width of the main beam. The parametric study covers the number of silicon perturbation, perturbation width, grating period, and the perturbation thickness. Effect of wavelength scanning on the antenna radiation characteristics is also addressed in this work. The results are based mainly on simulations obtained using the commercial software CST.

ISSN 2277-3061

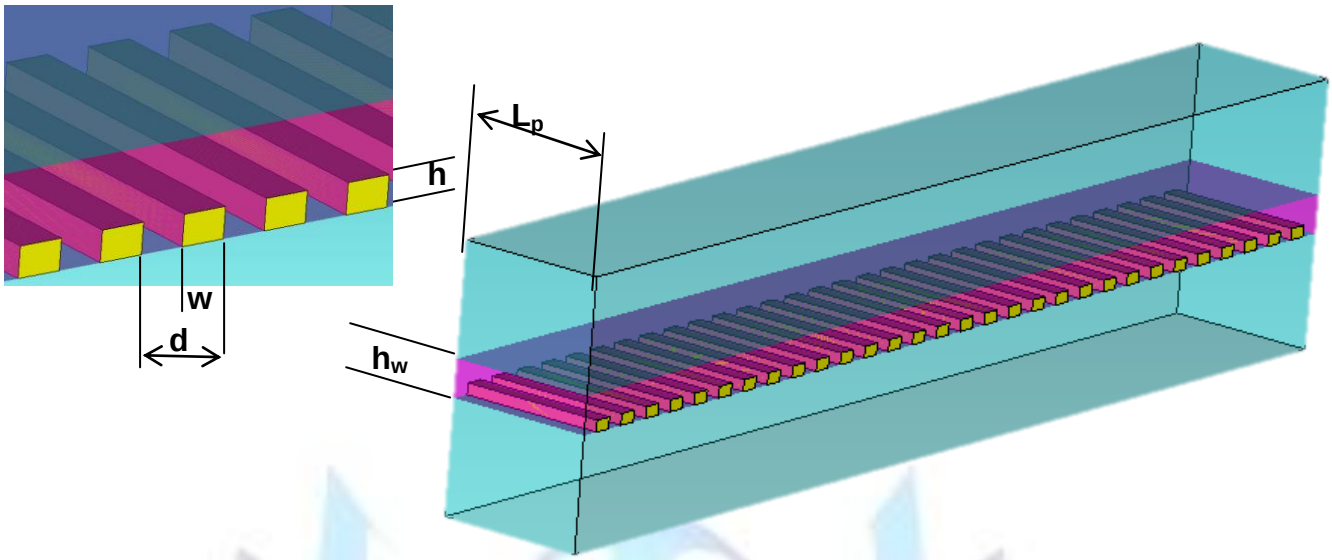

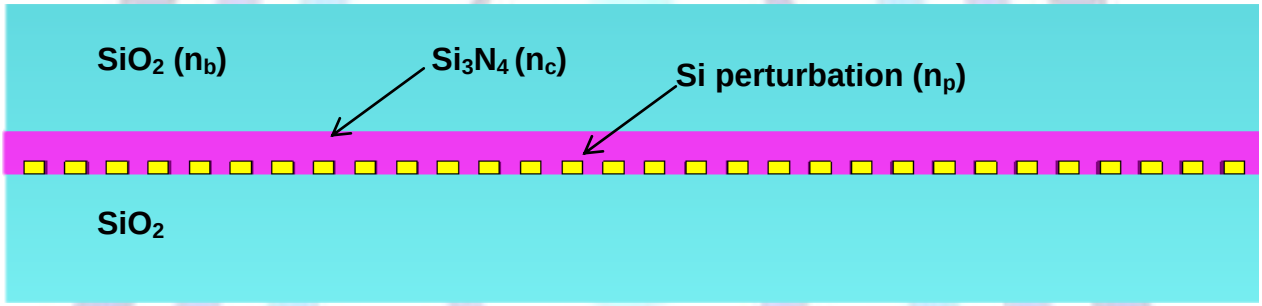

(b)

Fig 1: Silicon-based optical leaky wave antenna.
(a) Three-dimensional model.
(b) Two-dimensional model

2. STRUCTURE UNDER INVESTIGATION

Figures 1a and 1b show, respectively, the two-dimensional (2D) and three-dimensional (3D) models of the silicon OLWA under investigation. Note that the 2D model represents the lateral view of the 3D structure. The guiding structure has a dielectric core layer made of Si_3N_4 material and embedded between two SiO_2 cladding layers. The core is periodically corrugated by silicon bars which act as semiconductor perturbations. The refractive indices of the core, cladding, and perturbation are denoted by n_c, n_b, and n_p, respectively. At 1550 nm wavelength, $n_c=n_{Si3N4}=1.67$, $n_b=n_{SiO2}=1.45$, and $n_p= n_{Si}=3.48$.

The main geometrical features investigated in this study are

- Number of Si perturbations N
- Width of the Si bar w
- Thickness of the Si bar h
- Perturbation (grating) period d

The core thickness h_w and the length of the silicon bar L_p are fixed at 1000 nm and 4000nm, respectively.

When the waveguide is fed by a monochromatic optical source, the fundamental guided mode (axial mode) will be excited. The guided mode has an infinite set of space harmonics (also called Floquet waves [22, 24]. All the space harmonics have the same attenuation constant but have different propagation constant along the axial axis (z axis). The propagation constant of the n^{th} harmonic is given by

$$\beta_n = \beta_o + \frac{2\pi n}{d} \tag{1a}$$

$$= 2\pi[\frac{n_{eff}}{\lambda} + \frac{n}{d}] \tag{1b}$$

Where $\beta_o=n_{eff}k_o=n_{eff}(2\pi/\lambda)$ denotes the propagation constant of the fundamental mode with k_o denotes the vacuum wave number and n_{eff} is the effective refractive index. Harmonics with $|\beta_n|<\beta_b=n_bk_o$ are bounded (guided) waves and do not radiate (i.e., slow waves). To obtain leaky-wave radiation, fast waves (i.e., having $|\beta_n|>\beta_b$) must be excited.

Equation 1 can be used to determine the grating period d when the $-n^{th}$ propagation constant β_{-n} is known

$$d = \frac{2n\pi}{\beta_o - \beta_{-n}} \tag{2a}$$

$$d = \frac{n\lambda}{n_{eff} - n_b\left(\frac{\beta_{-n}}{\beta_b}\right)} \tag{2b}$$

Three values of d can be identified from eqn. 2b corresponding to $\beta_{-n}=0$, $\beta_{-n}=\beta_b$, $\beta_{-n}=-\beta_b$

$$d_{o(-n)} = n\lambda/n_{eff} \tag{3a}$$

$$d_{+(-n)} = n\lambda/(n_{eff} - n_b) \tag{3b}$$

$$d_{-(-n)} = n\lambda/(n_{eff} + n_b) \tag{3c}$$

Note that $d_{-(-n)} < d_{o(-n)} < d_{+(-n)}$. Note also that the $-n^{th}$ harmonic is a fast wave when the OLWA is fabricated with $d_{-(-n)} < d_{o(-n)} < d_{+(-n)}$.

When the silicon bar is designed with h=300 nm, w=0.5d, and λ=1550 nm, the CST simulation reveals that n_{eff}=1.538. Therefore, for the $n=-1$ harmonic, $d_{-(-1)}$=518.74 nm, $d_{o(-1)}$=1007.80 nm, and $d_{+(-1)}$=17613.64 nm=17.60 μm. These results reveal that $d_{+(-1)} >> d_{o(-1)}$ and $d_{-(-1)}$. For small-length LWA, one should design the antenna with 518.74 nm $<d<$ 1007.8 nm leading to $\beta_{-1}/\beta_b<-1$ which ensures a fast wave in the backward direction.

Its worth to examine the possibility of exciting $n=-2$ leaky-wave harmonic under the above design constraint. For $n=-2$ harmonic, $d_{-(-2)}$=1037.48 nm, $d_{o(-2)}$=2015.6 nm, $d_{+(-2)}$=35.23 μm.Note that $d_{-(-2)} > d_{o(-1)}$ which ensures that $n=-2$ harmonic does not contribute to the radiation when the LWA is designed with $d<d_{o(-1)}$.

The radiated angle with respect to the broadside θ can be computed from the relation $\cos\theta = \beta_{-1}/\beta_b$[19,22]. This leads to

$$\cos\theta = \frac{1}{n_b}[n_{eff} - \frac{\lambda}{d}] \tag{4a}$$

$$d = \frac{\lambda}{n_{eff} - n_b\cos\theta} \tag{4b}$$

where eqn.1 has been used. At $d=d_o=\lambda/n_{eff}$, $\theta=-\pi/2$ operating with $d_{-(-1)}<d<d_{o(-1)}$ will shift θ from the $-\pi/2$ reference.

Let $\theta=(-\pi/2)+\theta_{shift}$, then

$$sin\,\theta_{shift} = \frac{1}{n_b}[n_{eff} - \frac{\lambda}{d}] \quad (5a)$$

$$d = \frac{\lambda}{n_{eff} - n_b\, sin\,\theta_{shift}} \quad (5b)$$

$$\cong \frac{\lambda}{n_{eff} - n_b\,\theta_{shift}} \quad \text{when the absolute value of } \theta_{shift} \text{ is less than } \pi/2 \quad (5c)$$

Note that θ_{shift} is negative when $d<d_{o(-1)}$according to eqn.5a.

Let the OLWA is designed with $d=d_{o(-1)}-\Delta d$, then eqn.5b reduces to

$$\Delta d = \frac{\lambda}{neff}\left[1 - \frac{1}{\left(1 - \frac{n_b}{n_{eff}}\sin\theta_{shift}\right)}\right] \quad (6a)$$

or

$$\frac{\Delta d}{d_{o(-1)}} = 1 - 1/(1 - \frac{n_b}{n_{eff}}\sin\theta_{shift}) \quad (6b)$$

For θ_{shift}=-2.5^o for example, $\Delta d/d_{o(-1)}$=0.04, Therefore, the antenna should be designed with d= 967.5 nm.

Figure 2a shows the variation of the normalized propagation constant of the *n=-1* harmonic (β_{-1}/β_b) and *n=-2* harmonic (β_{-2}/β_b) with perturbation period *d*. the corresponding direction of the radiated beam is given in Fig. 2b.

In the following section, the results ate presented for d=976.5 nm antenna by simulating the 3D model using CST. Unless otherwise stated, the following parameter values are used in the simulation

λ=1550 nm, h=300nm, h_w=1000 nm, d=970 nm, w=0.5d=485 nm, L_p=29585 nm.

3. PARAMETRIC STUDY

The aim of this section is to investigate the effect of various parameters on the performance of the LWA. Unless otherwise stated, the parameter values used in the simulation are wavelength λ=1550 nm, silicon perturbation period d=967.5 nm, perturbation length d_1=d/2=485 nm, perturbation thickness h=300 nm, and waveguide thickness w=1000 nm. The waveguide length L is set equal to N_d, where N is the number of silicon perturbations.

3.1. Effect of number of perturbations

Figures 4-9 show the effect of number of silicon perturbations N on the farfield radiation characteristics of the antenna. Each figure is plotted for a specific value of N and contains four parts. Part (a) illustrates the three-dimensional (3D) farfield radiation pattern, while parts (b)-(d) show the radiation patterns in the yz, xy, and xz planes, respectively. Note that the narrow beam radiation is satisfied for all values of N considered here (N=10-60).

The spectra of the scattering patterns S_{11} and S_{21} are displayed in Figures 10a-f for N=10, 20,… 60, respectively. Investigating these figures reveals that both S_{11} and S_{21} are less than -20 dB over the wavelength 1400-1700 nm for all values of N. If the power attenuation in the waveguide is mainly due to wave radiation, then the incident (input) power can be split into three components, $P_{in}=P_r+P_t+P_{rad}$. The reflected power $P_r=S_{11}^2\ P_{in}<0.01P_{in}$ and the transmitted power $P_t=S_{11}^2P_{in}<0.01P_{in}$. This leaves $P_{rad}>0.98P_{in}$ as a radiated power. These results indicate that high radiation efficiency is expected even when the LWA is designed with N=10. However, the presence of intrinsic waveguide loss reduces the efficiency below 0.98.

The results in Figure 10 also indicate that the scattering parameter S_{11} is less sensitive to number of silicon perturbations; this result is expected since S_{11} depends mainly on the interface between the environment and the waveguide input. This point can be discussed further by calculating approximately the average refractive index of the waveguide core.

$$n_{av} = \frac{[h\,n_{Si} + (w - h)n_{Si3N4}]d_1 + w\,n_{Si3N4}\,(d - d_1)}{d\,w}$$

$$= \left(\frac{h}{w}\right)\left(\frac{d_1}{d}\right)n_{Si} + [1 - \left(\frac{h}{w}\right)\left(\frac{d_1}{d}\right)]n_{Si3N4} \quad (7)$$

For h=300 nm, w=1000 nm, n_{Si}=3.48, and n_{Si3N4}=1.67, n_{av} is estimated to be 1.94. The power reflection from air (n=1) to the waveguide is $R = \left(\frac{n_{av}-n}{n_{av}+n}\right)^2$ = 0.1 (-10 dB).

Figure 11 presents the variation of the scattering parameters S_{11} and S_{21} with the number of silicon perturbations at 1550 nm wavelength. Note that when N exceeds 30, S_{11} saturates at -33 dB.

The dependence of antenna radiation parameters on number of silicon perturbations is illustrated further in Figures 12a-g for 1550nm wavelength. These figures show, respectively, the efficiency, directivity, gain, main lobe magnitude, main lobe direction, side lobe level, and the 3dB angular width of the main mode. The radiation parameters for N=10, 20….,60 are listed in Table 1. Investigating these figures and Table 1 reveals the following findings.

(i) Both radiation efficiency and total efficiency are increasing functions of N and this effect is more pronounced for N<10 where the efficiency increases almost linearly with N. For N>10, the efficiency varies slowly with N and tends to saturate as N approaches 60. At N=30, the total and radiation efficiencies are 0.82 and 0.87, respectively. These values are to be compared with 0.86 and 0.89, respectively, when N=60. These results can be explained as follows. The variation of the radiation power along the waveguide can be expressed as

$$P_{rad}(z) = \frac{\propto_{rad}}{\propto_{in} + \propto_{rad}} P_{in}\, e^{-(\propto_{in} + \propto_{rad})\, z} \tag{8}$$

where$\propto_{in}$ and $\propto_{rad}$ are the attenuation coefficients due to intrinsic loss and radiation loss, respectively. At the end of the waveguide z=Nd and the total radiated power

$$P_{rad} = \frac{\propto_{rad}}{\propto_{in} + \propto_{rad}} P_{in}[1 - e^{-(\propto_{in} + \propto_{rad})Nd}] \tag{9}$$

For small values of N, where$(\propto_{\mathrm{in}} + \propto_{\mathrm{rad}})\mathrm{Nd} \ll 1$, $e^{-(\propto_{\mathrm{in}} + \propto_{\mathrm{rad}})\mathrm{Nd}}] \cong 1 - (\propto_{\mathrm{in}} + \propto_{\mathrm{rad}})\mathrm{Nd}$. Then the radiation power $\mathrm{P_{rad}}/P_{in} = \propto_{\mathrm{rad}} \mathrm{Nd}$. This leads to an efficiency increasing linearly with N. When N is large such that$(\propto_{\mathrm{in}} + \propto_{\mathrm{rad}})\mathrm{Nd} \gg 1$, then $\mathrm{P_{rad}}/P_{in} \cong \propto_{\mathrm{rad}}/(\propto_{\mathrm{in}} + \propto_{\mathrm{rad}})$, which is independent of N.

(ii) The magnitude of the main (side) lobe is an increasing (decreasing) function of N and tends to a saturated level when N exceeds 30. The magnitude of the main lobe is 36.76, 45.53, and 46.77 dB, respectively, for N=10, 20, and 60. The corresponding magnitude of the side lobe is -3.20, -9.30, and -9.10, respectively.

(iii) The direction of the main lobe is almost independent of N for N >6.

(iv) The 3dB angular width of the main lobe decreases with increasing N and this effect is more pronounced for N<10. For N>10, the beam width decreases slightly with N and tends to saturate as N approaches 60. The beam width is 7.50^{o}, 3.00^{o}, and 2.10^{o} for N=10, 30, 60, respectively

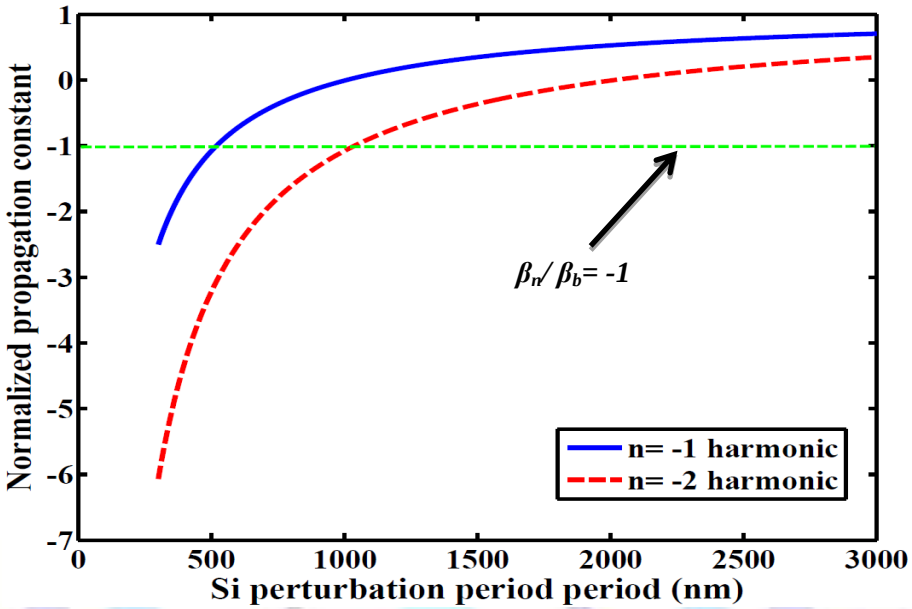

Fig 2: Normalized propagation constant for the n=-1 and n=-2 harmonics.

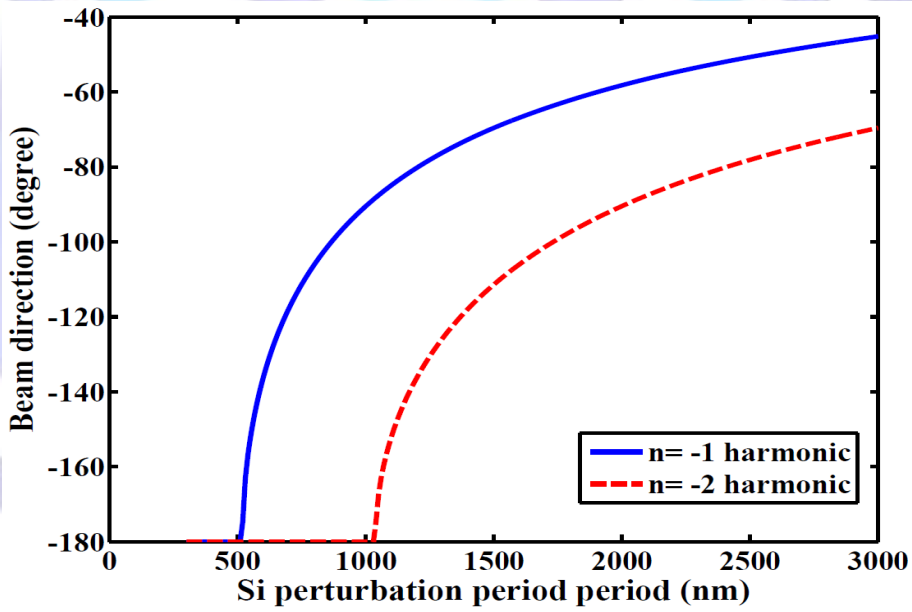

Fig 3: Variation in the direction angle of the n=-1 and n=-2 harmonics with perturbation period.

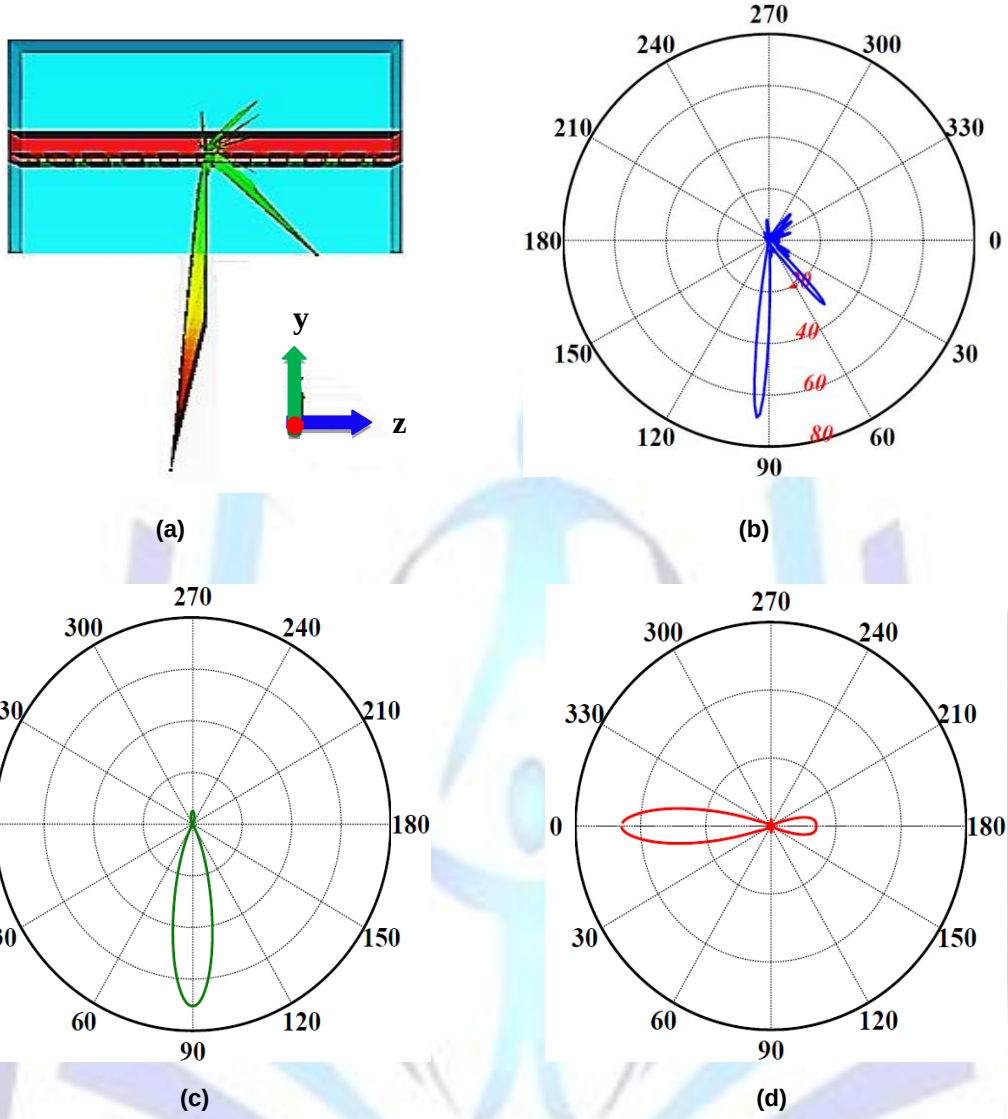

Fig 4: Farfield characteristics for N=10.

(a) 3D farfield pattern (b) yz plane (c) xy plane (d) xz plane.

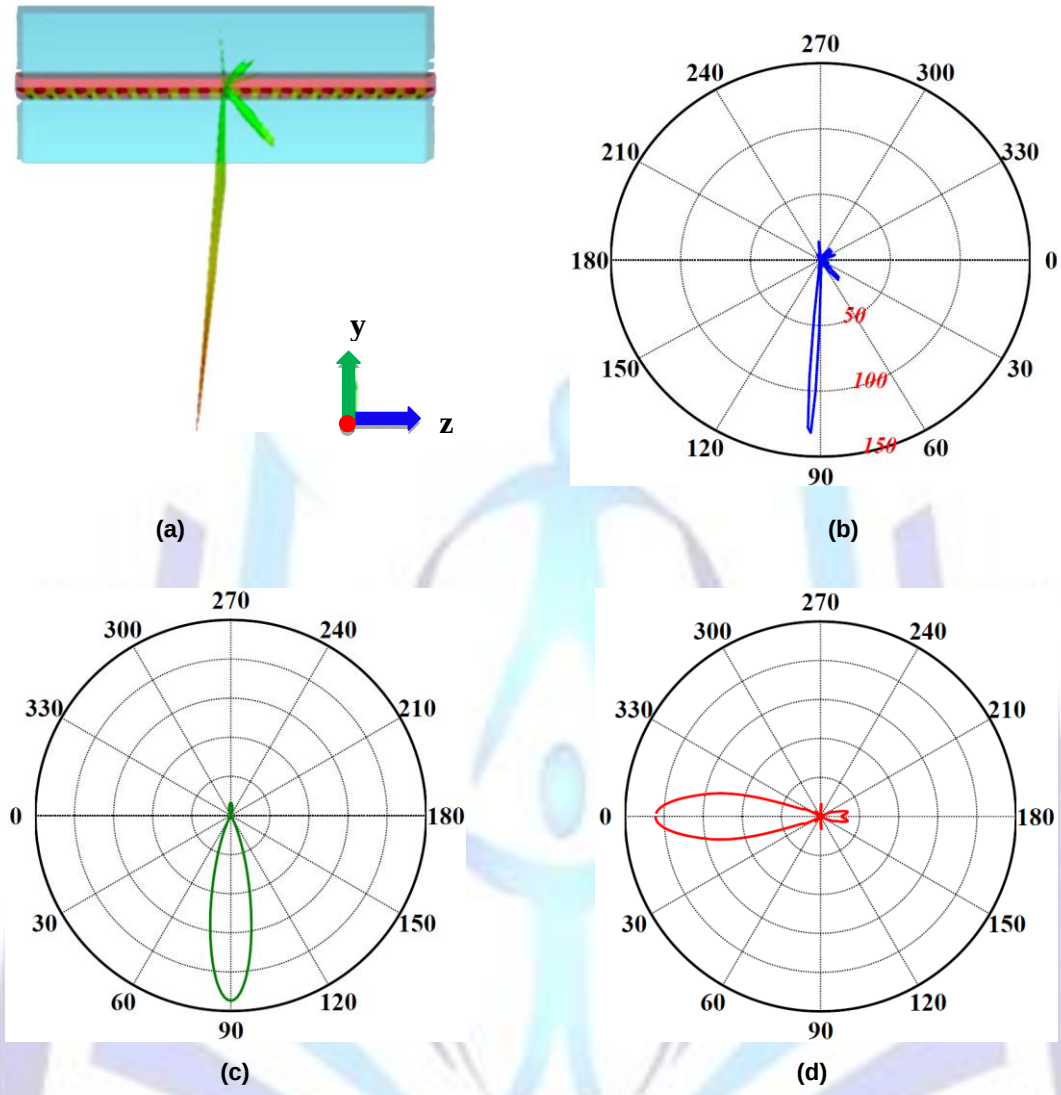

Fig 5: Farfield characteristics for N=10.

(a) 3D farfield pattern (b) yz plane (c) xy plane (d) xz plane.

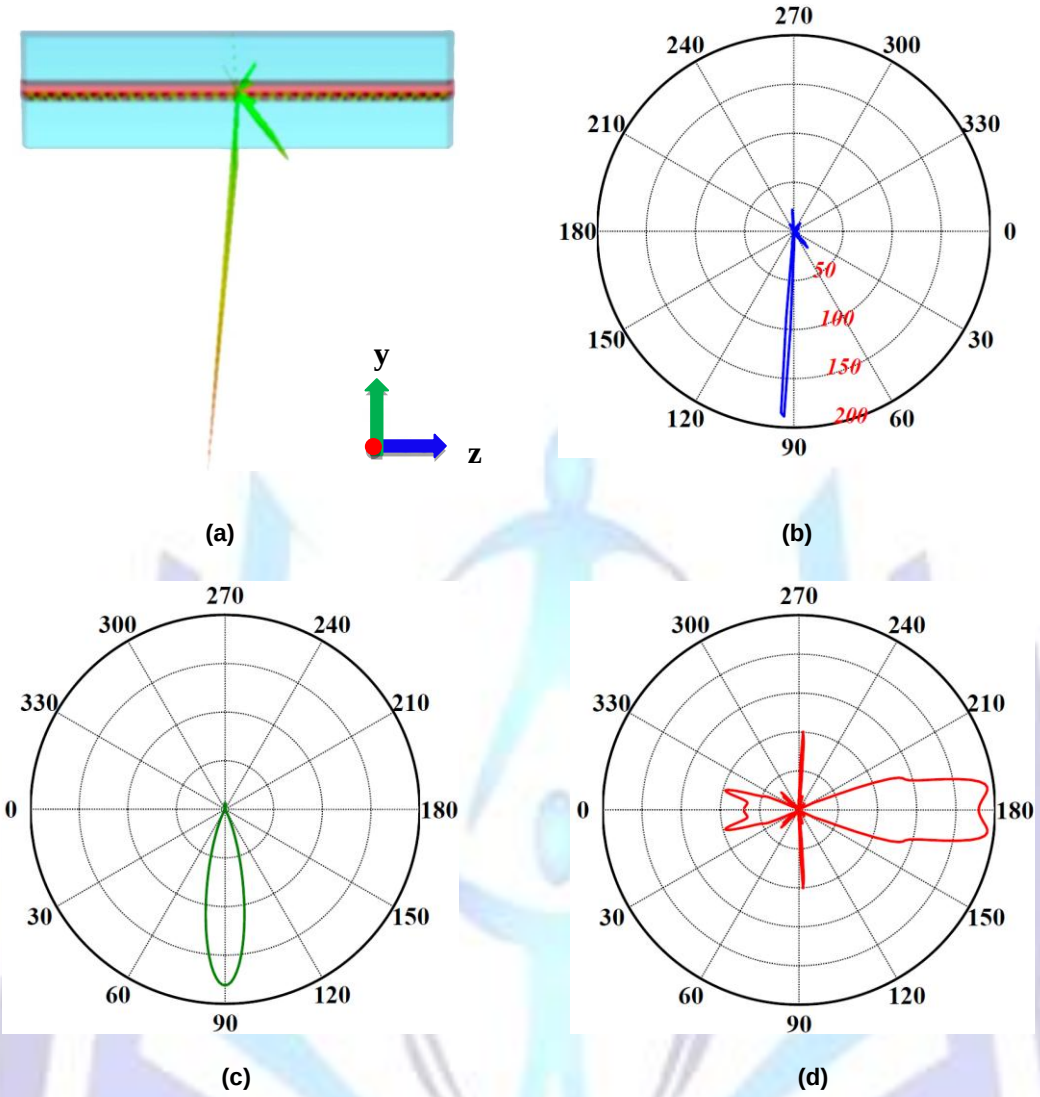

Fig 6: Farfield characteristics for N=10.

(a) 3D farfield pattern (b) yz plane (c) xy plane (d) xz plane.

ISSN 2277-3061

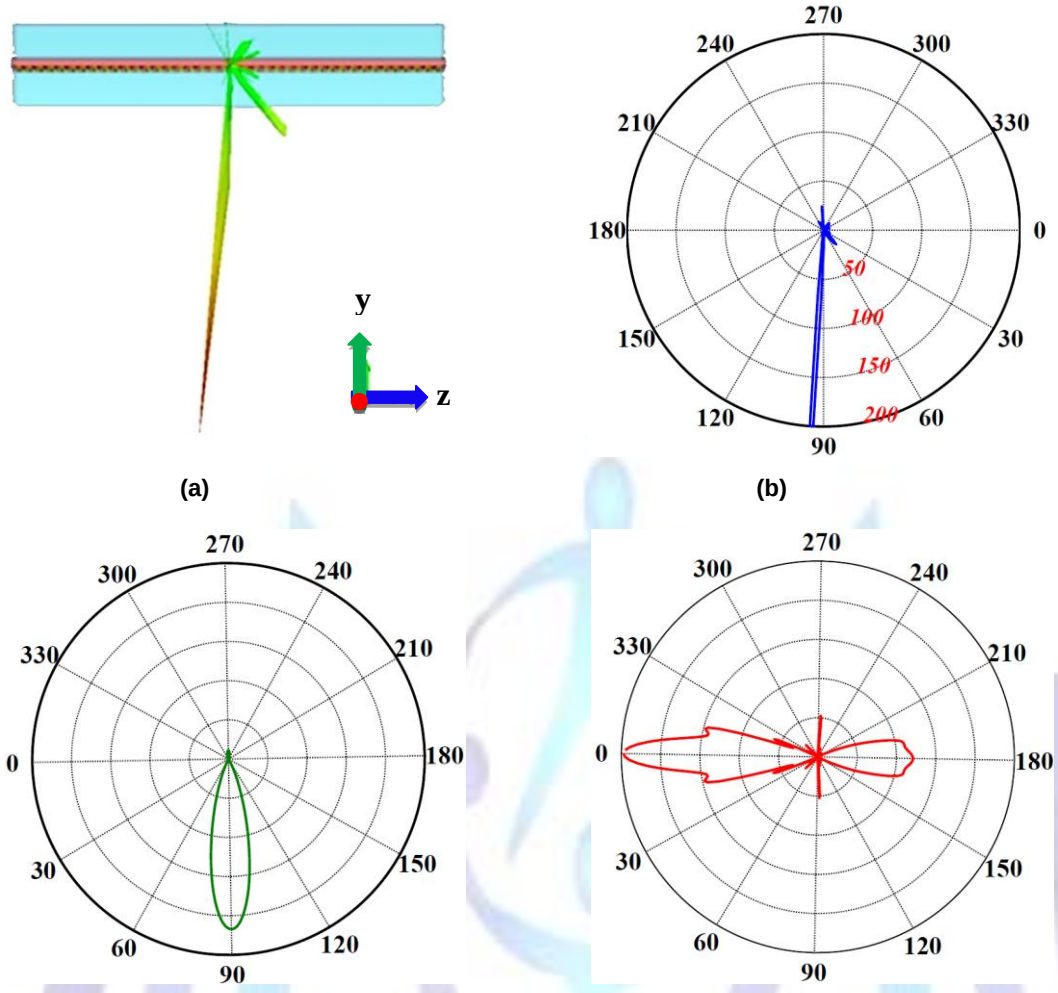

Fig 7: Farfield characteristics for N=10.

(a) 3D farfield pattern (b) yz plane (c) xy plane (d) xz plane.

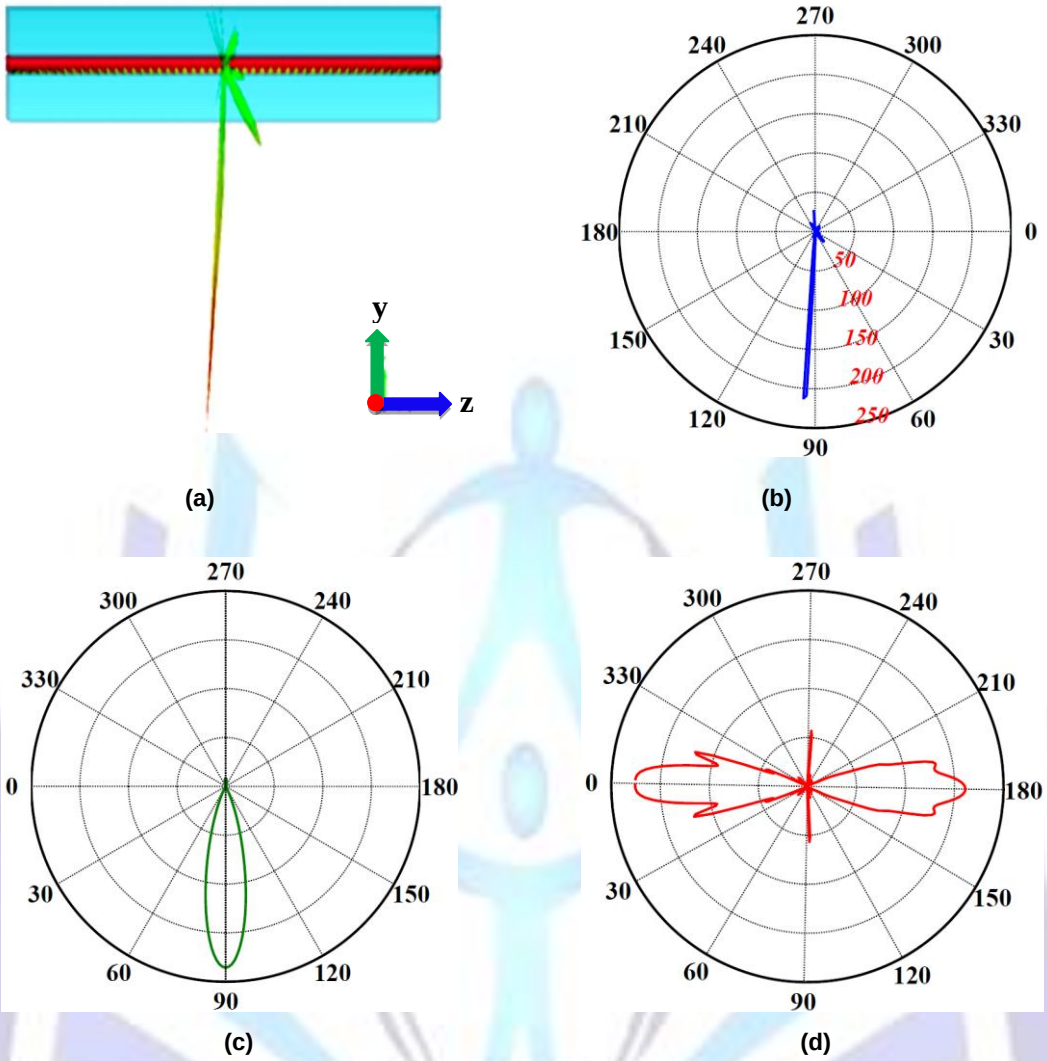

Fig 8: Farfield characteristics for N=10.

(a) 3D farfield pattern (b) yz plane (c) xy plane (d) xz plane.

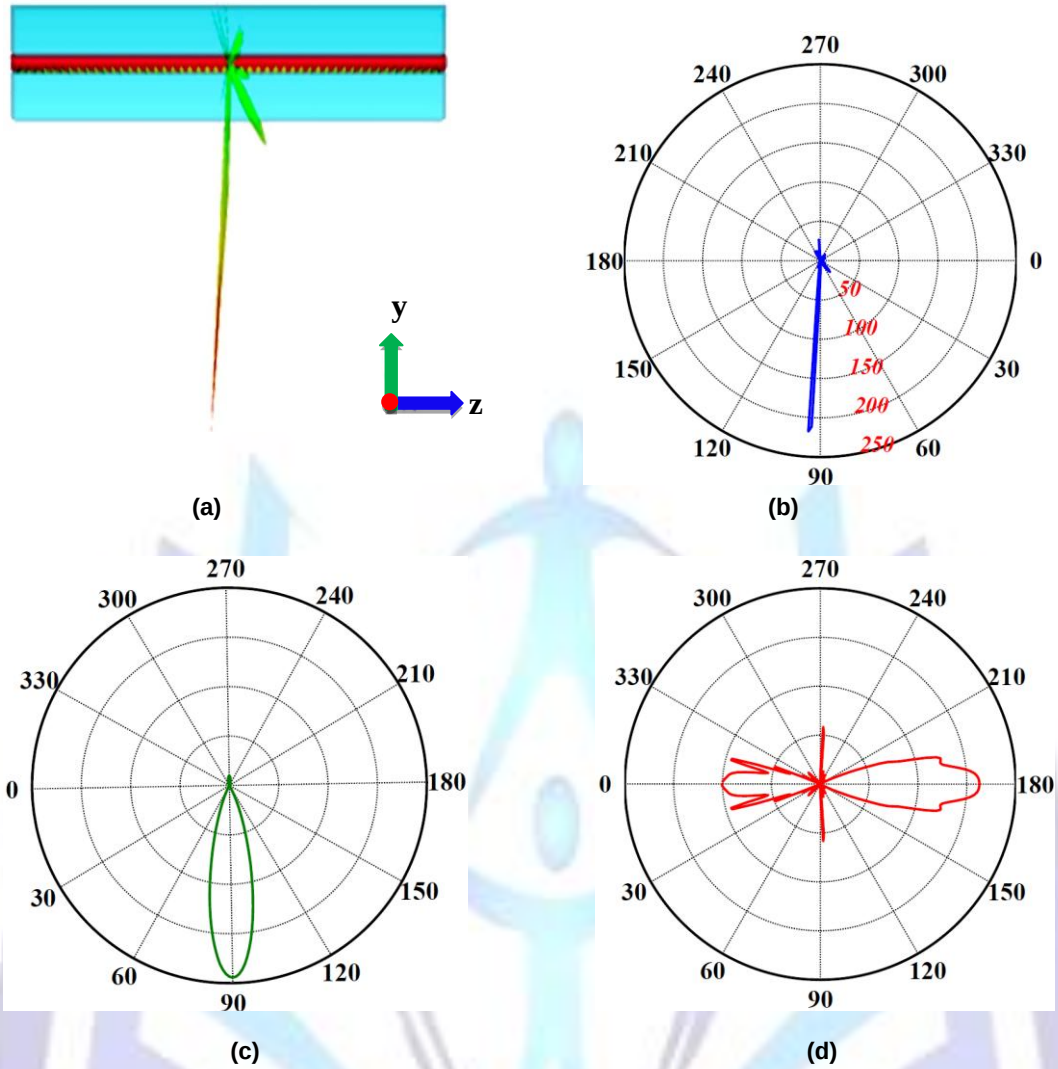

Fig 9: Farfield characteristics for N=10.

(a) 3D farfield pattern (b) yz plane (c) xy plane (d) xz plane.

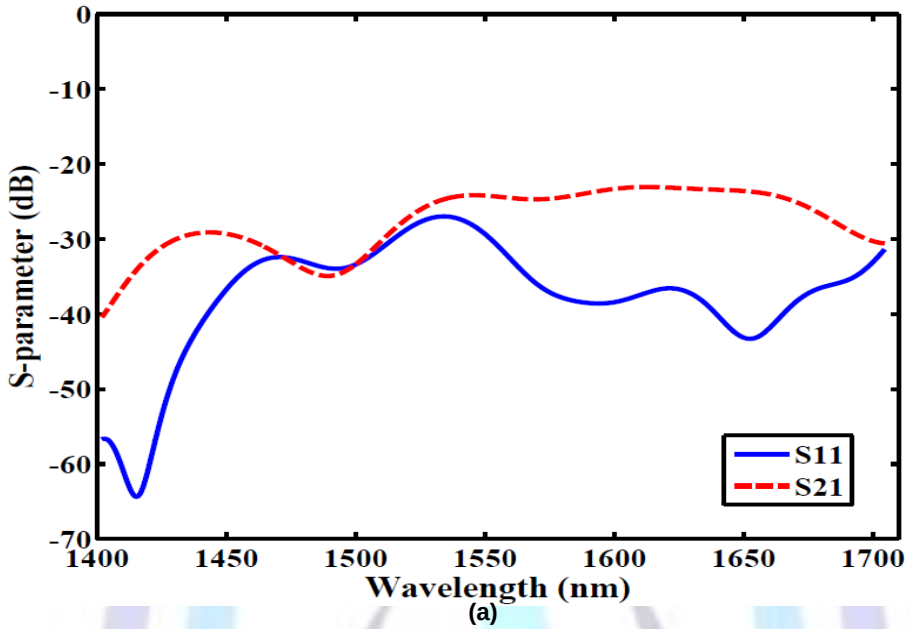

(a)

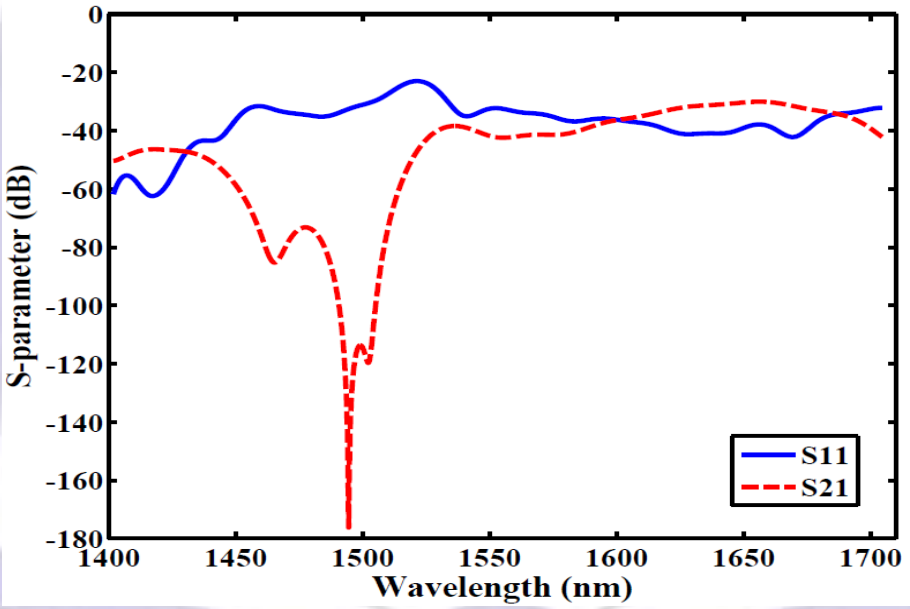

(b)

Fig 10: Variation of scattering parameters, S_{11} and S_{21} with wavelength for different numbers of silicon perturbations (a) N=10 (b) N=20 (c) N=30 (d) N=40 (e) N=50 (f) N=60.

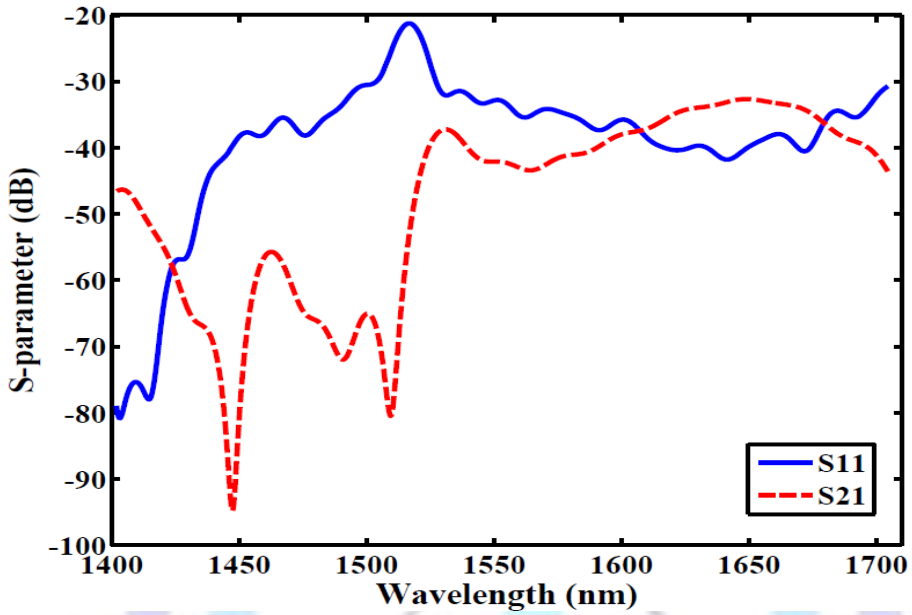

(c)

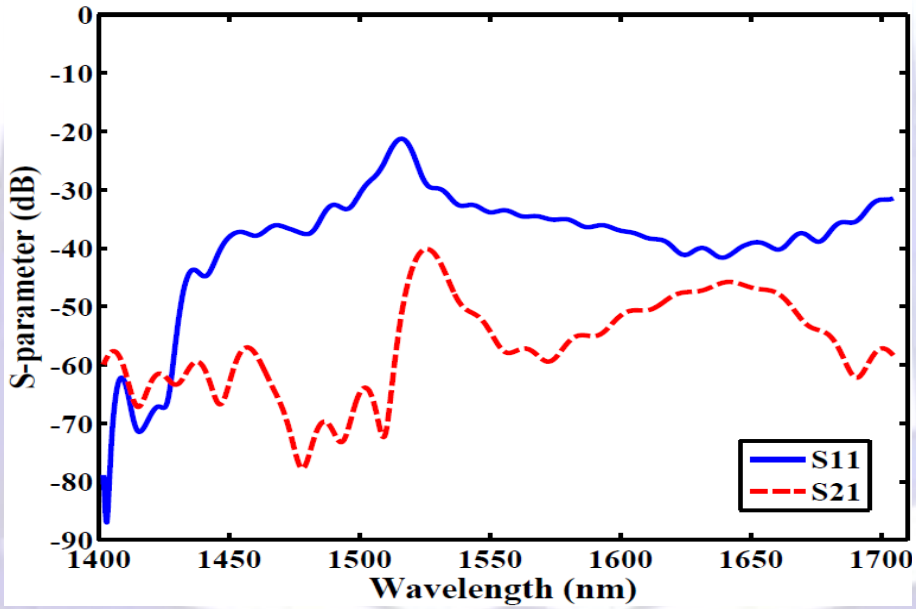

(d)

Fig 10: (Continued).

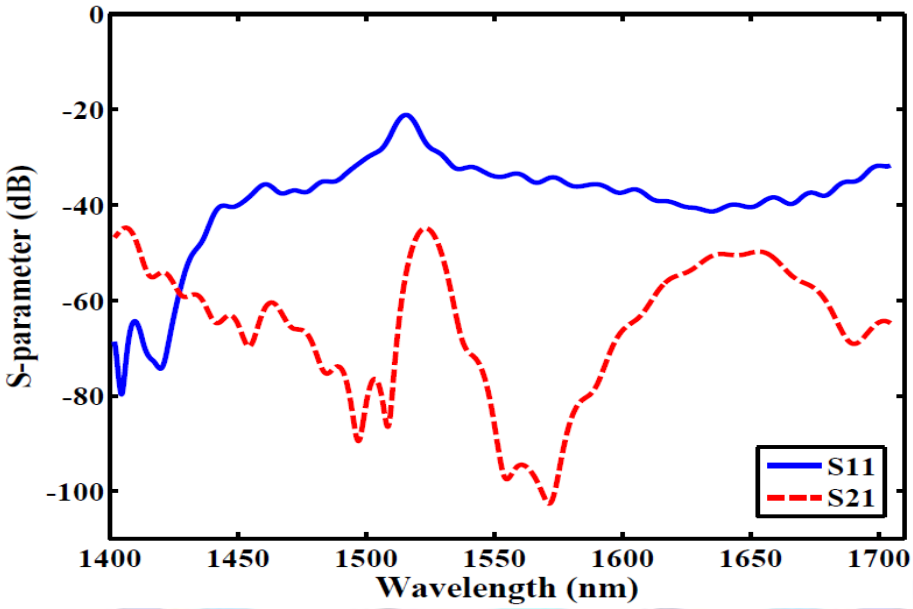

(e)

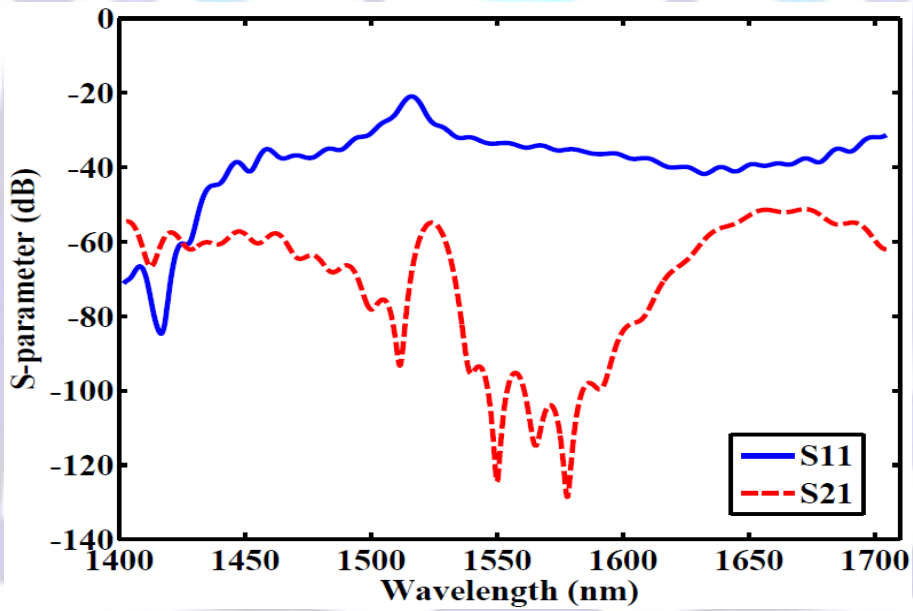

(f)

Fig 10: (Continued).

ISSN 2277-3061

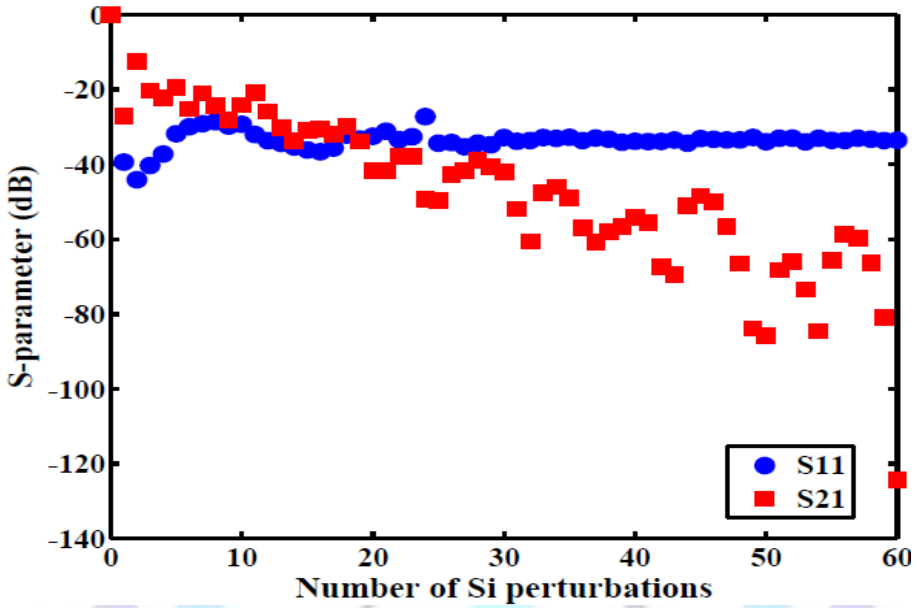

Fig 11: Dependence of the scattering parameters on the number of silicon perturbations.

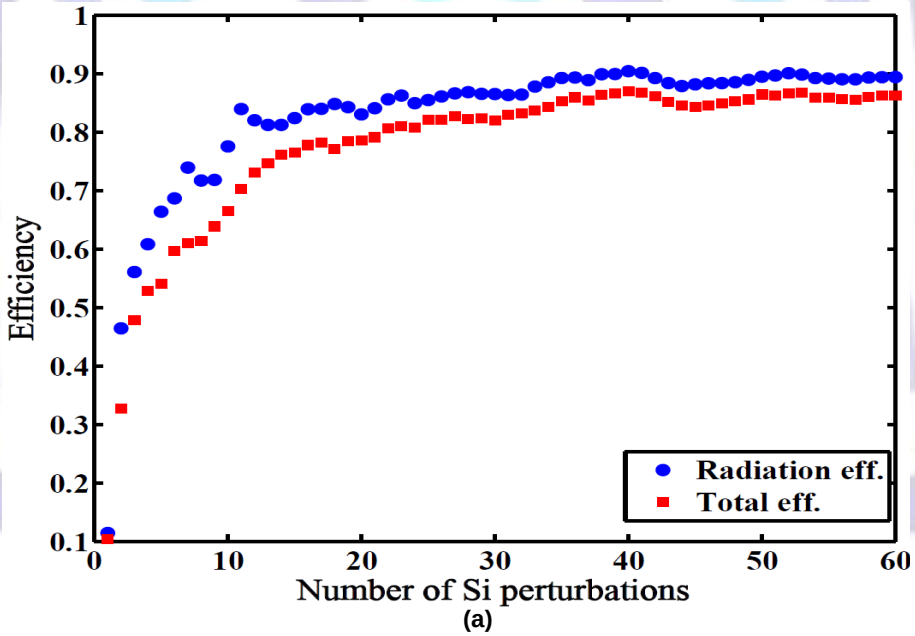

(a)

Fig 12 :Dependence of radiation parameters on the number of silicon perturbations (a) efficiency (b) directivity (c) gain (d) main lobe magnitude (e) main lobe direction (f) side lobe level (g) 3 dB angular width.

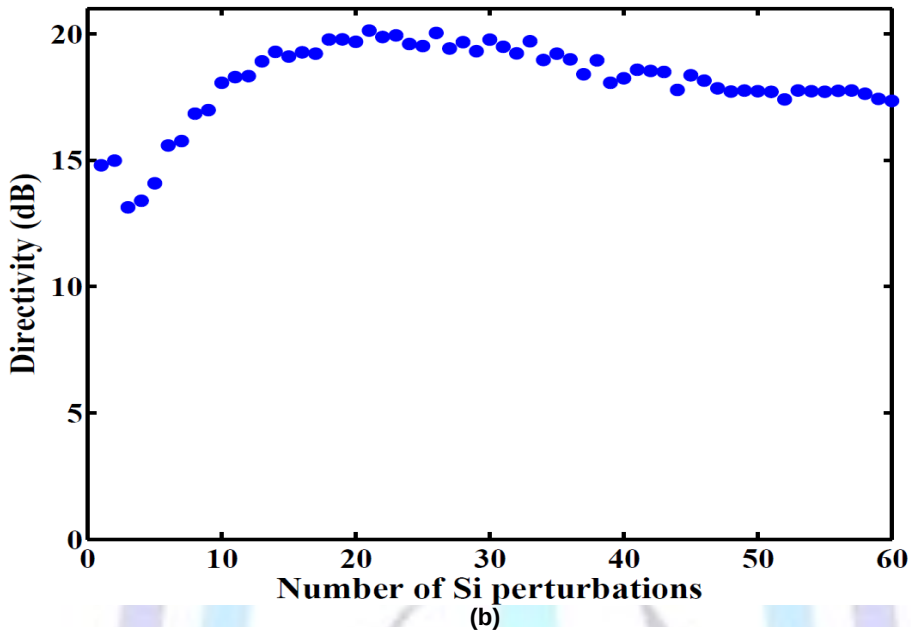

(b)

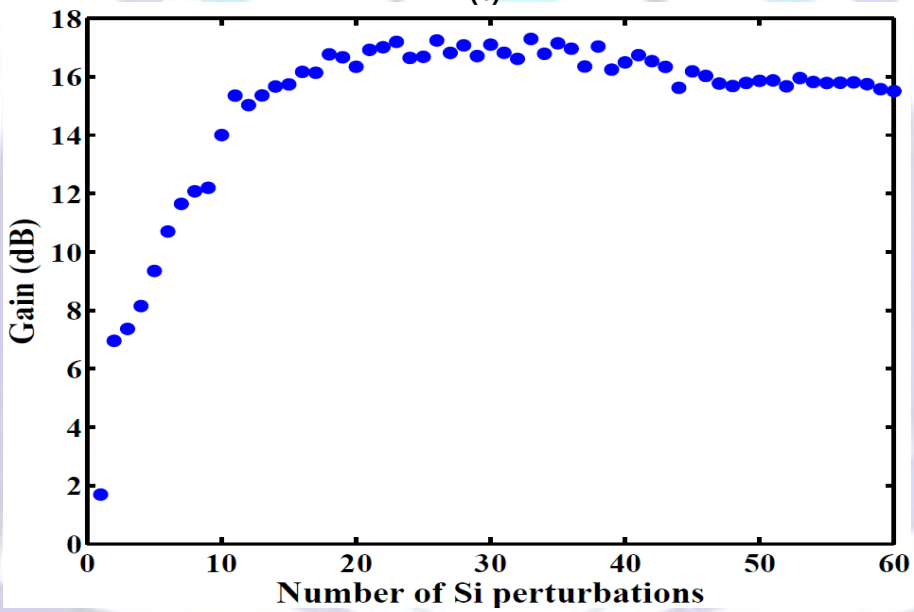

(c)

Fig 12: (Continued).

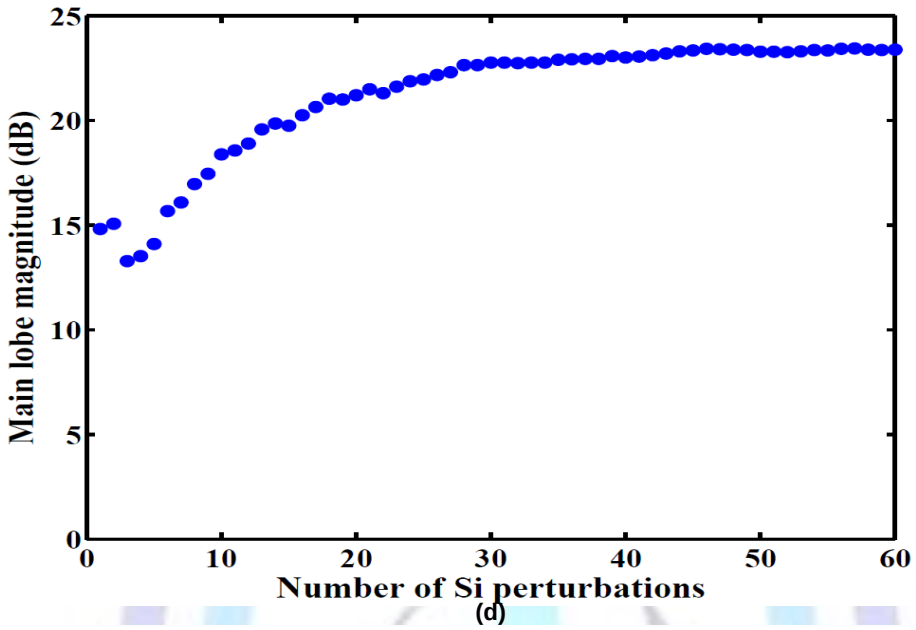

(d)

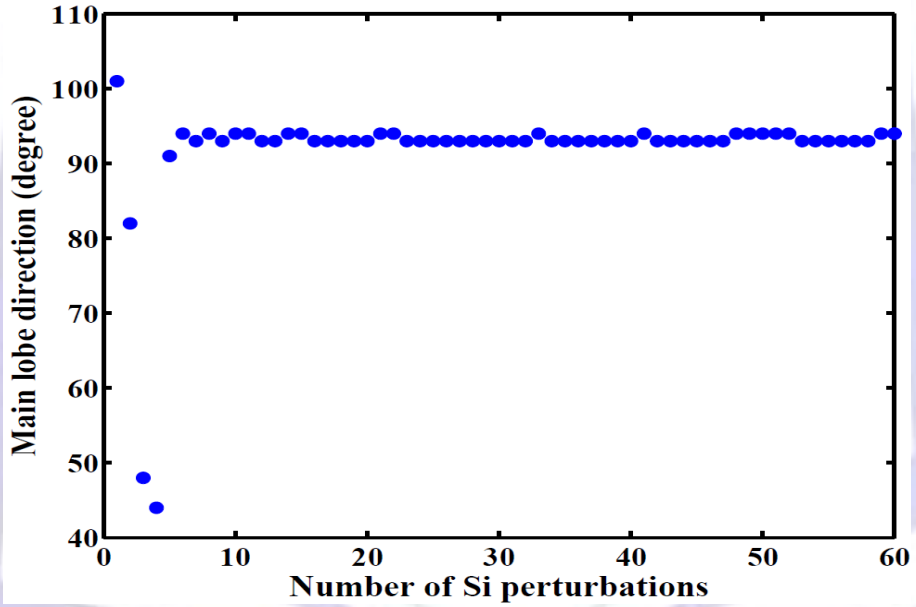

(e)

Fig 12: (Continued).

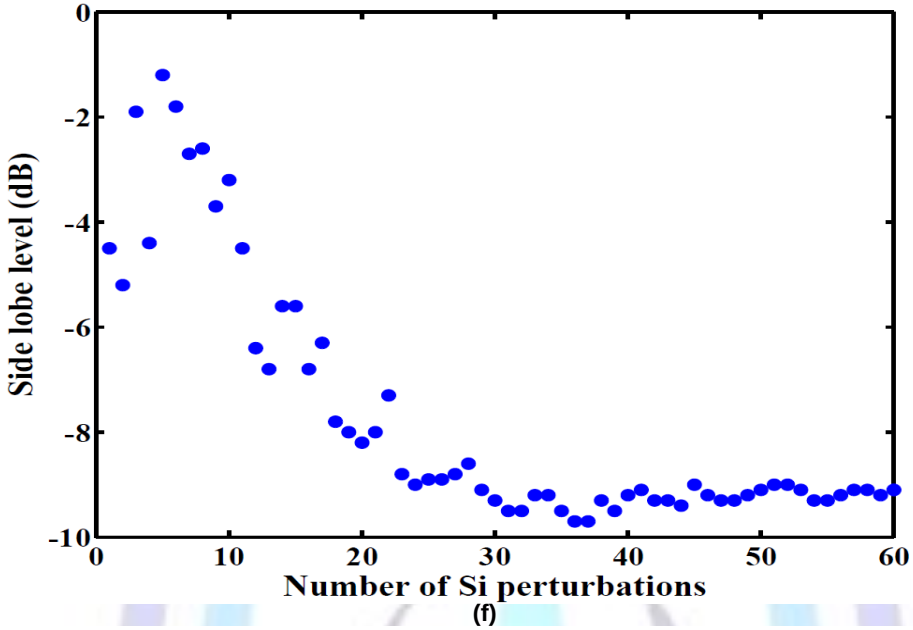

(f)

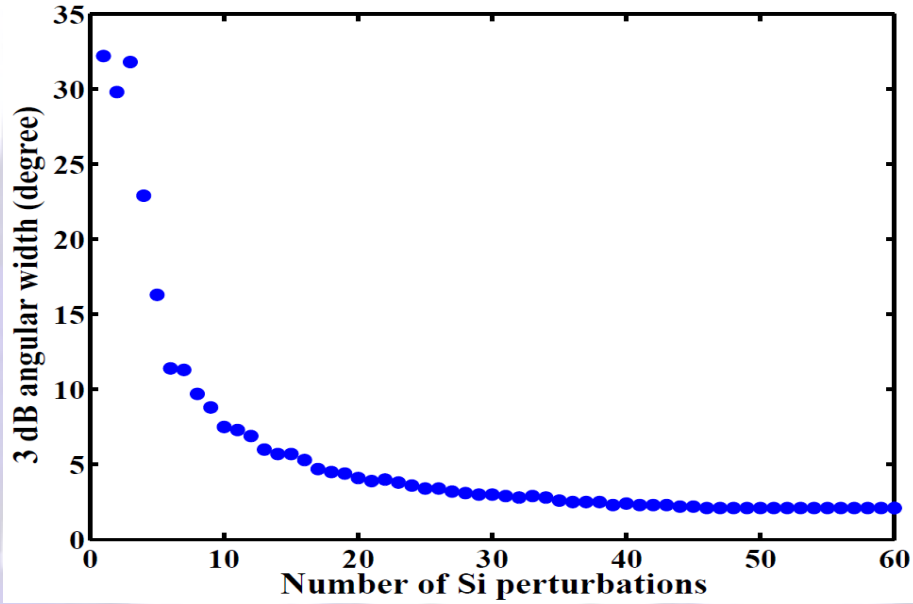

(g)

Fig 12: (Continued).

Table1.Dependence of antenna radiation parameters on number of silicon perturbations

	Number of silicon perturbations					
Radiation parameter	**10**	**20**	**30**	**40**	**50**	**60**
$\|S_{11}\|$ (dB)	-12.74	-14.11	-14.27	-14.71	-14.76	-14.59
$\|S_{21}\|$ (dB)	-10.51	-18.16	-18.29	-23.57	-37.29	-54.02
Radiation efficiency	0.78	0.83	0.87	0.90	0.89	0.89
Total efficiency	0.67	0.79	0.82	0.87	0.86	0.86
Directivity (dB)	41.85	45.32	94.75	66.69	59.24	54.25
Gain (dB)	32.24	37.62	39.36	37.97	36.51	35.70
Main lobe magnitude	68.90	132.00	189.00	200.00	213.00	218.00
Main lobe direction (degree)	94.00	93.00	93.00	93.00	94.00	94.00
Side lobe level (dB)	-3.20	-8.20	-9.30	-9.20	-9.10	-9.10
3dB angular width (degree)	7.50	4.10	3.00	2.40	2.10	2.10

3.2. Effect of silicon bar width

The effect of silicon bar width won the radiation pattern characteristics are presented in Figures 13a-h for N=30 and λ=1550 nm. The silicon bar widthis varied from w=0 nm (corresponding to the absence of silicon perturbations) to w=d=976.5 nm (corresponding to a 300 nm thick silicon layer deposited along the waveguide). Table2 lists the radiation parameters for different values of w which lie around the point under observation (w=483.75 nm).

Table2. Effect of silicon bar width w on the antenna radiation parameters for λ=1550 nm and N=30.

Radiation parameter	**Silicon bar width (nm)**				
	400	**450**	**475**	**500**	**550**
S_{11} (dB)	-13.27	-13.68	-14.29	-14.47	-11.03
S_{21} (dB)	-21.41	-19.09	-18.27	-18.79	-22.05
Radiation efficiency	0.87	0.86	0.86	0.87	0.73
Total efficiency	0.82	0.81	0.82	0.83	0.67
Directivity (dB)	21.42	21.30	19.77	19.40	13.18
Gain (dB)	18.6	18.32	17.00	16.88	9.61
Main lobe magnitude (dB)	22.74	23.03	22.76	22.74	22.41
Main lobe direction (degree)	94.00	94.00	93.00	93.00	93.00
Side lobe level (dB)	-12.10	-11.20	-9.30	-8.30	-5.30
3dB angular width (degree)	3.00	2.80	3.00	2.80	2.90

Two main conclusions can be drawn from these results.

- The radiation parameters vary slowly with bar width in the region around w=483.75 nm. This region extends from 300-550 nm for most radiation parameters.
- In the region 300-550 nm, the optimum value of w depends on the required radiation parameter to be optimized. For example maximum gain of 18.32 dB occurs when w= 450 nm. Other optimum values are listed in Table 3.

Table3. Optimum radiation parameters in the region around 483.75 nm

Radiation parameter	Optimum value	Corresponding optimum value of silicon bar width (nm)
Radiation efficiency	0.88	300
Total efficiency	0.85	300
Directivity (dB)	21.49	350
Gain (dB)	18.90	350
Main lobe magnitude (dB)	23.03	450
Main lobe Direction (degree)	93	483.75,500,550
Side lobe level (dB)	-12.10	400
3dB angular width (degree)	2.80	450,500

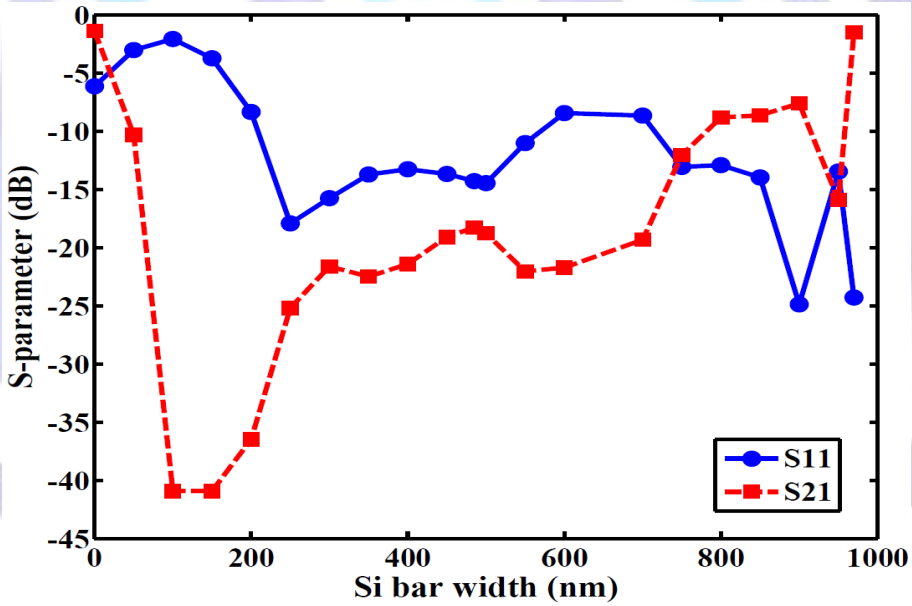

(a)

Fig 13: Variation of radiation parameters with silicon bar width (a) S-parameter (b) efficiency (c) directivity (d) gain (e) main lobe magnitude (f) main lobe direction (g) side lobe level (h) 3 dB angular width.

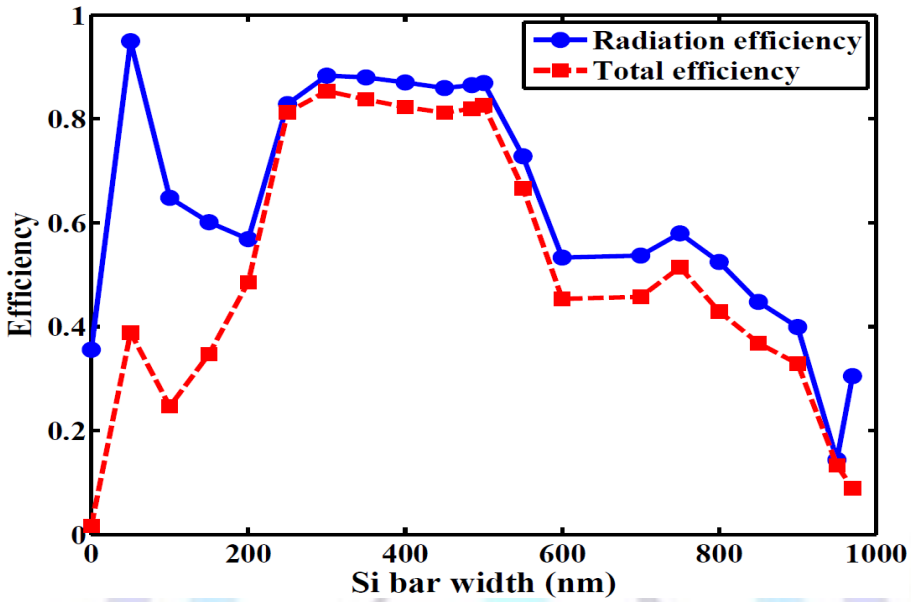

(b)

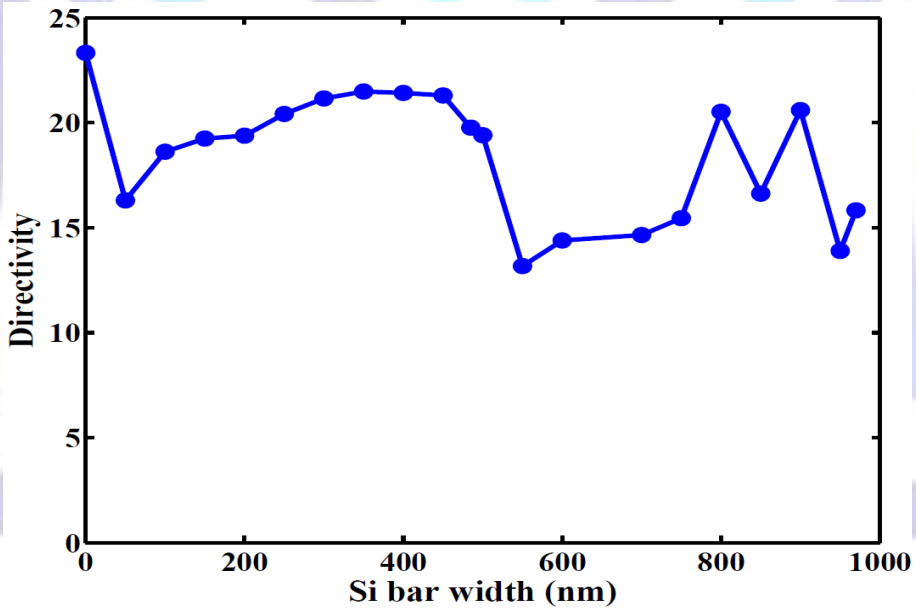

(c)

Fig 13: (Continued).

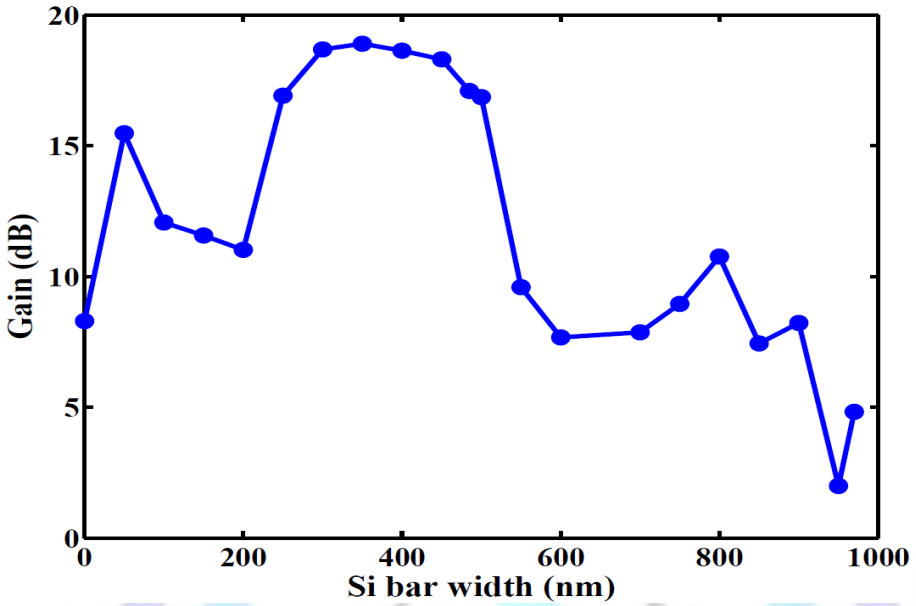

(d)

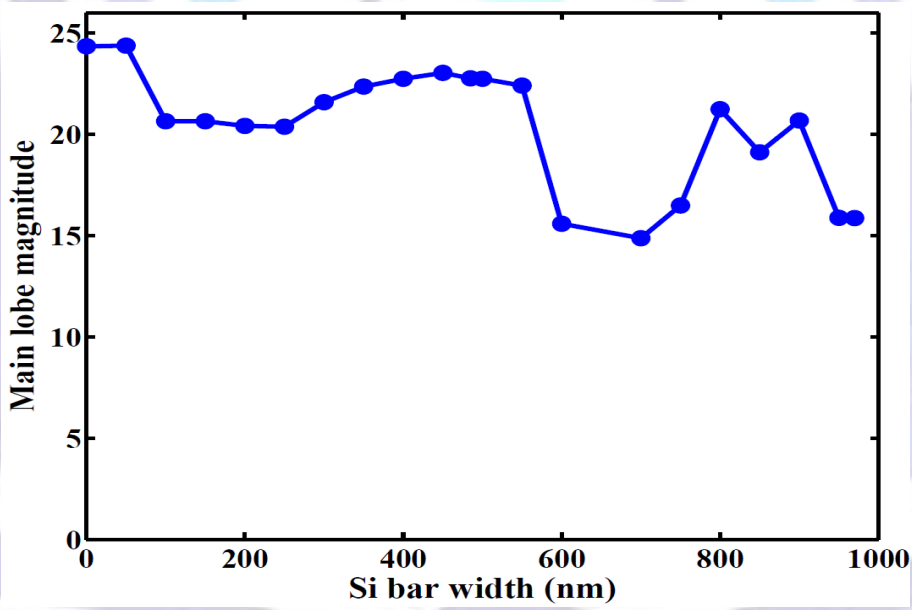

(e)

Fig 13: (Continued).

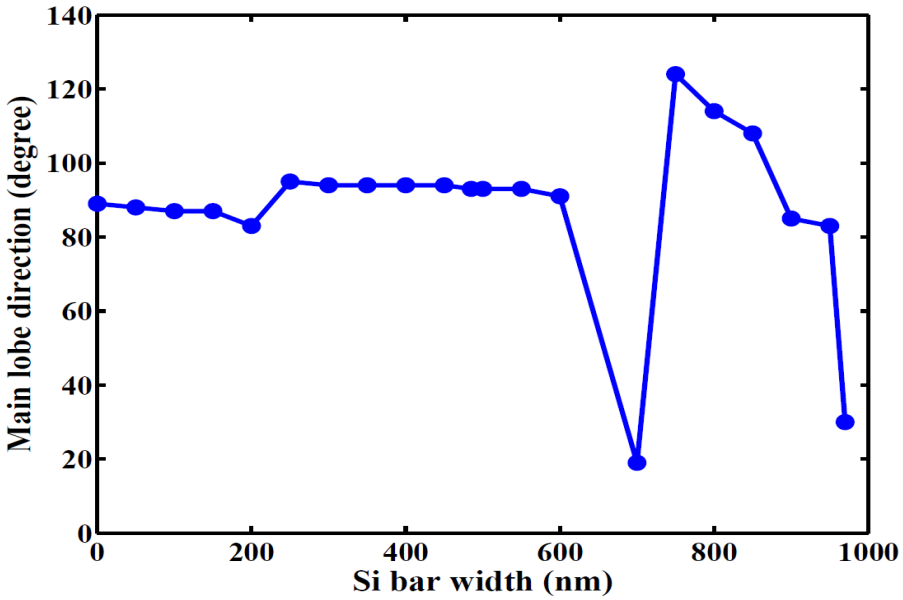

(f)

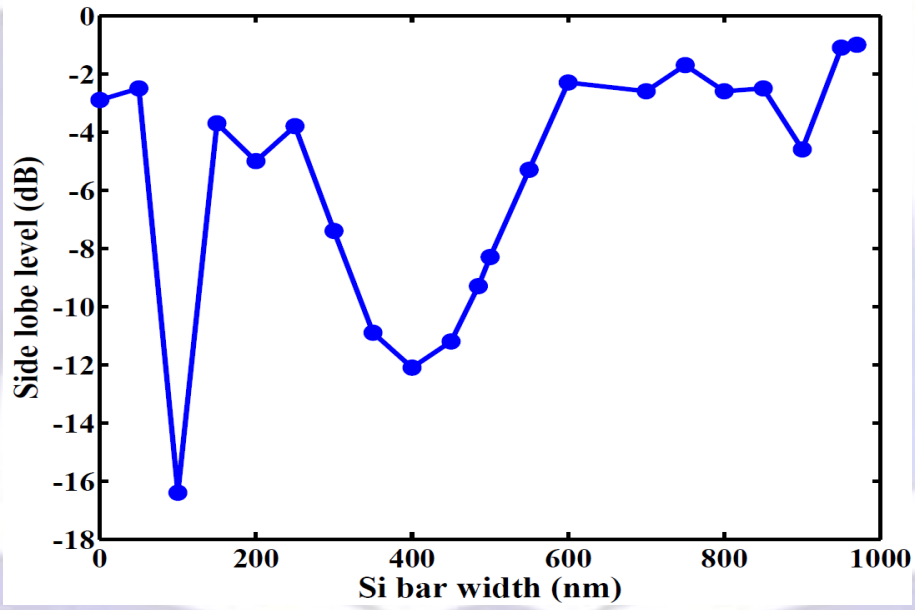

(g)

Fig 13: (Continued).

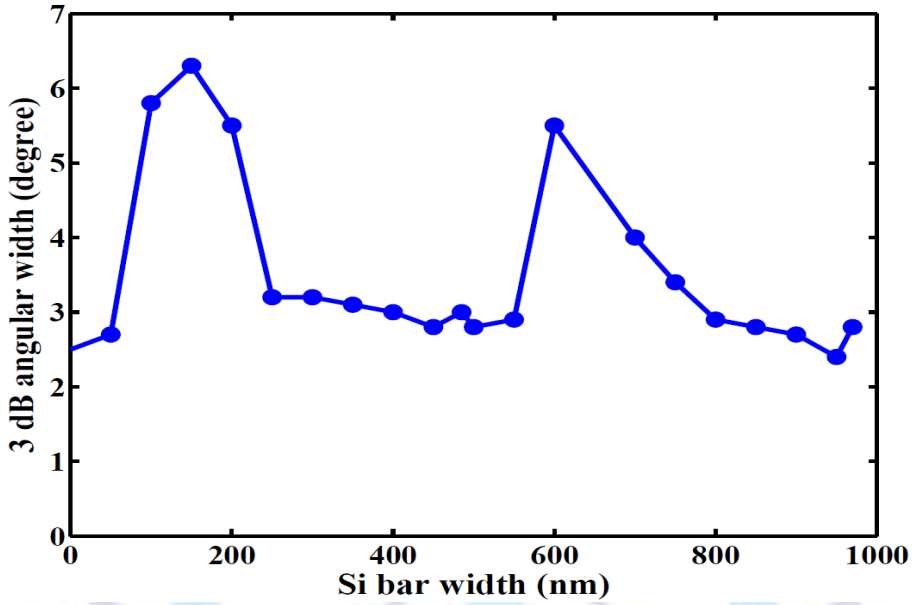

(h)

Fig 13: (Continued).

3.3. Effect of silicon bar thickness

The variation of radiation characteristics with the silicon bar thickness h is also investigated and the results are displayed in Figures 14a-h for N=30 and λ=1550 nm. In these figures, the bar thickness is varied from h=0 nm (corresponding to the absence of silicon perturbations) to $h=h_w$=1000 nm. Table 4 summarizes the main radiation properties for different values of h around the point of interest (h=300 nm). Note that very good radiation characteristics is obtained when the LWA is designed with h=300 nm. At this point, the total efficiency is maximum (≅0.82), the radiation efficiency is as high as 0.87, and the 3dB angular beam width is as narrow as 3.00°.

Table4. Effect of silicon bar thickness on the radiation parameters for λ=1550 nm and N=30.

Radiation parameter	Silicon bar thickness (nm)						
	225	250	275	300	325	350	375
S_{11}(dB)	-15.43	-15.09	-14.90	-14.29	-13.36	-20.97	-22.72
S_{21}(dB)	-11.77	-14.56	-17.69	-18.34	-21.65	-28.66	-16.73
Radiation efficiency	0.83	0.85	0.87	0.87	0.81	0.70	0.74
Total efficiency	0.75	0.80	0.82	0.82	0.77	0.70	0.72
Directivity (dB)	19.50	20.41	20.40	19.77	14.43	14.80	15.38
Gain (dB)	16.17	17.35	17.75	17.20	11.67	10.36	11.39
Main lobe magnitude (dB)	22.55	23.18	23.08	22.77	20.86	15.92	15.66
Main lobe direction (degree)	94.00	94.00	94.00	93.00	92.00	46.00	46.00
Side lobe level (dB)	-3.50	-6.80	-9.20	-9.30	-6.70	-2.90	-2.80
3dB angular width (degree)	2.60	2.70	2.80	3.00	2.70	8.50	6.10

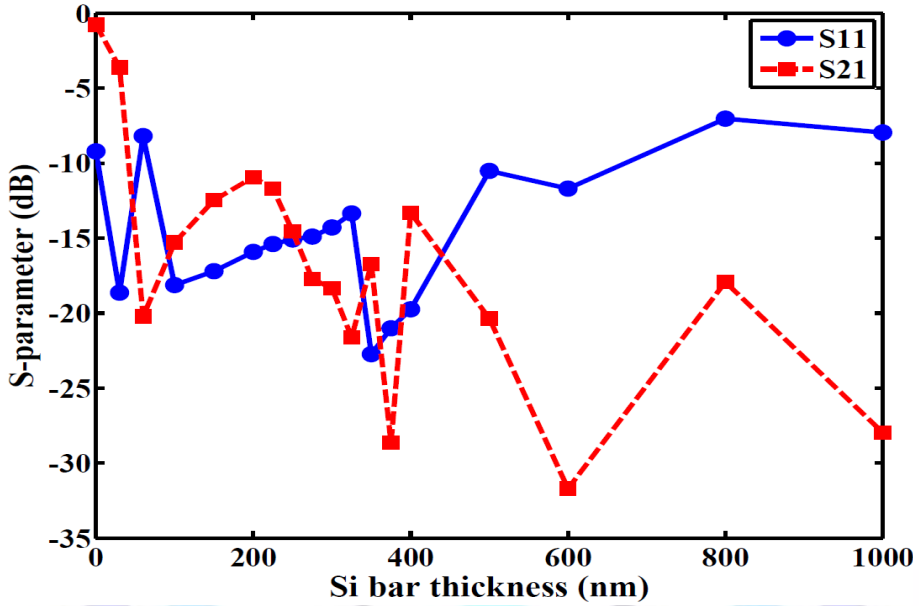

(a)

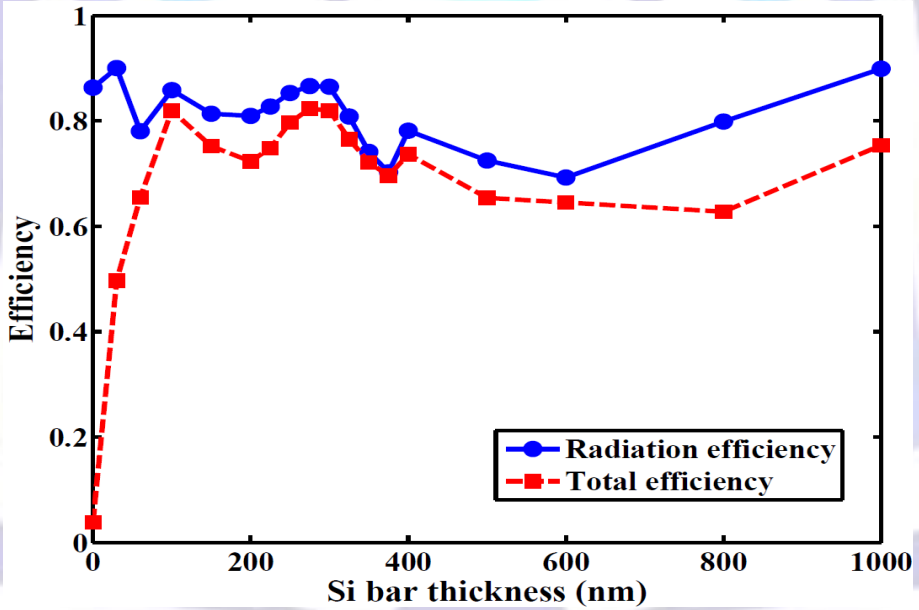

(b)

Fig 14: Variation of radiation parameters with silicon bar thickness (a) S-parameter (b) efficiency (c) directivity (d) gain (e) main lobe magnitude (f) main lobe direction (g) side lobe level (h) 3 dB angular width.

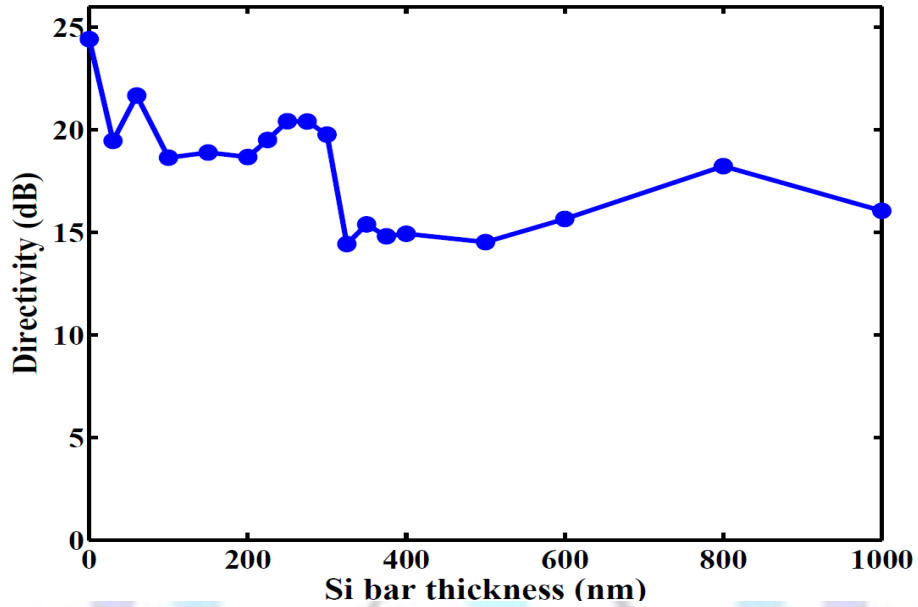

(c)

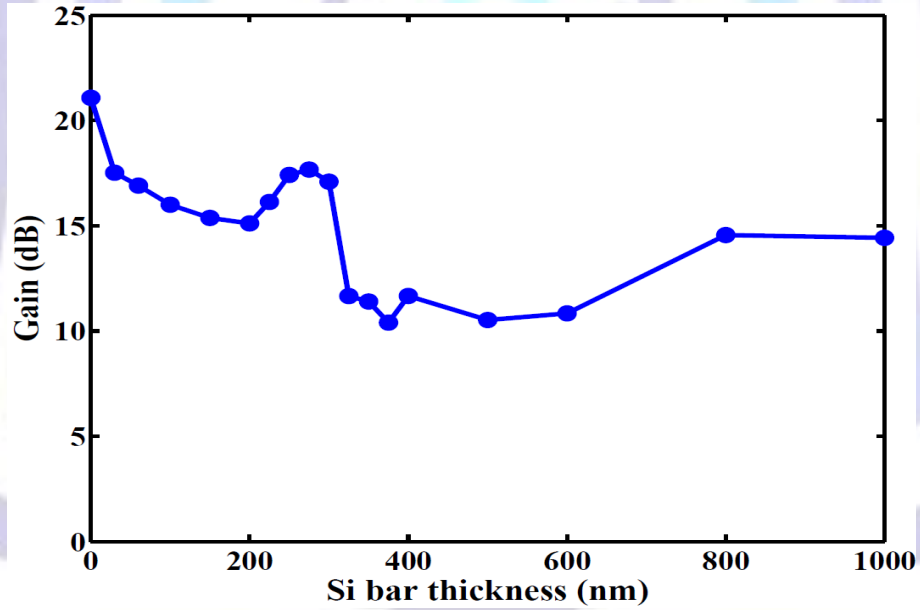

(d)

Fig 14: (Continued).

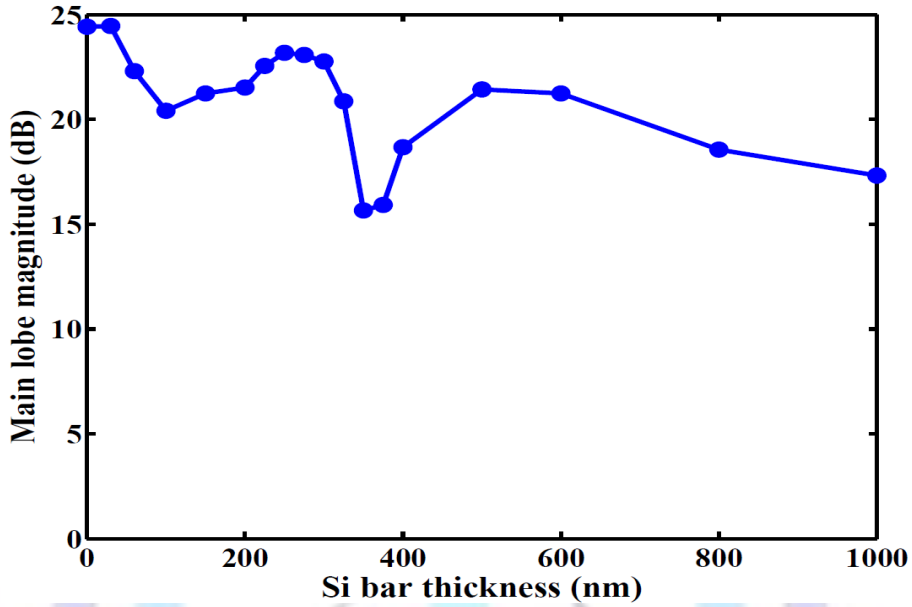

(e)

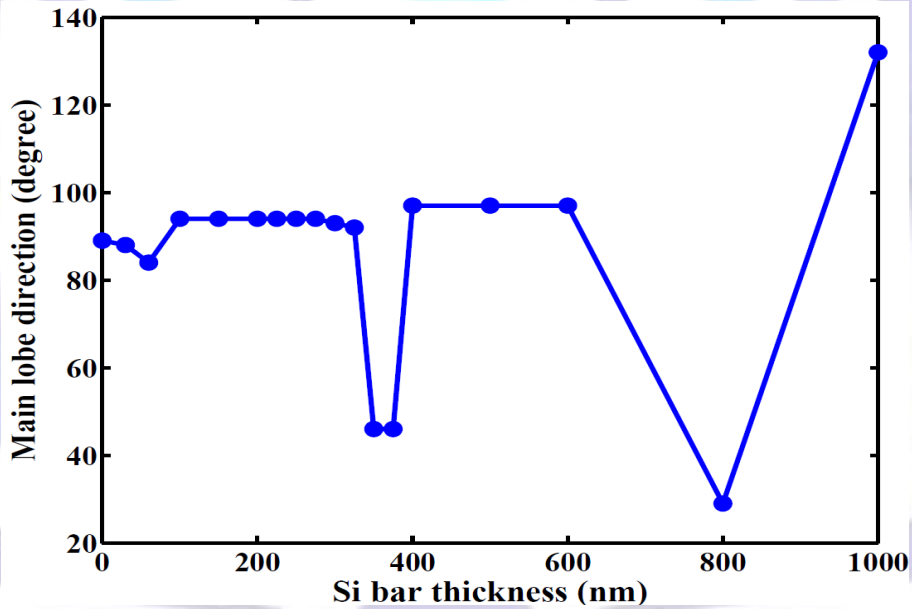

(f)

Fig 14: (Continued).

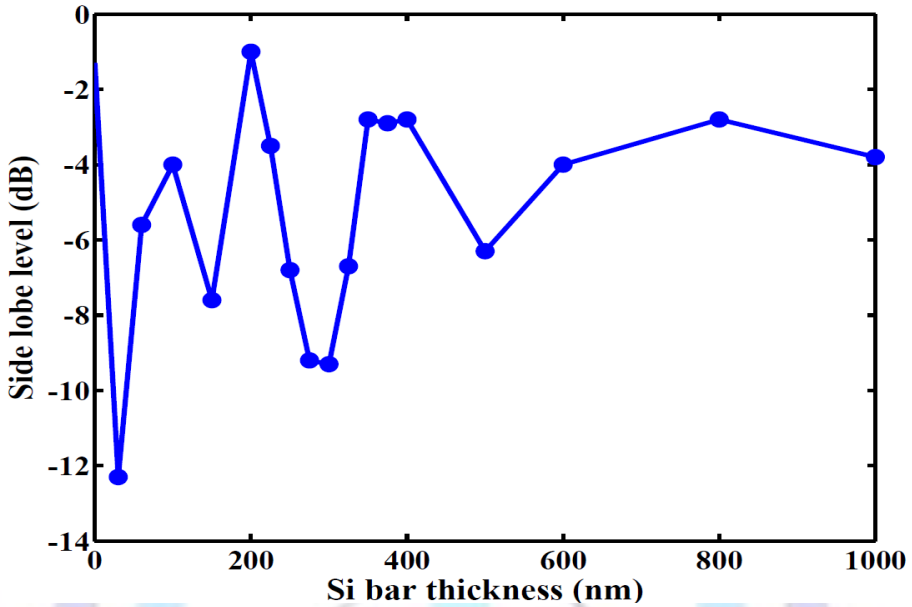

(g)

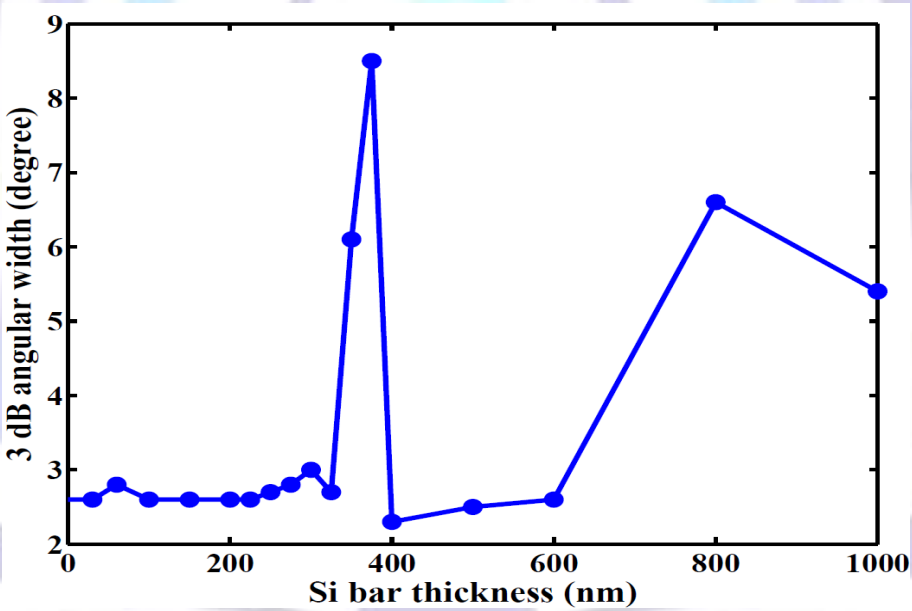

(h)

Fig 14: (Continued).

3.4. Effect of grating period

Figures15 a-h show the variation of pattern characteristics with the silicon perturbation period d when the LWA is designed with w/d=0.5 for 1550 nm operation.

Table 5 lists the radiation parameters for different values of d chosen around the point of observation (i.e., d=967.5 nm). Note that designing the antenna with d=976.5 nm will maximize directivity (19.77 dB), radiation efficiency (0.86), total efficiency (0.82), gain (17.09 dB), and main lobe magnitude (19.69 dB). Note further that both S_{11} and S_{21} are both less than -15 dB at this value of grating period.

An interesting finding can be drawn from Figure 15f which shows decreasing of the main lobe direction θ_{out} with increasing grating period. The data here fits perfectly the following relation

$$\theta_{out}\,(degree) = a + b/d\,(nm) \tag{10}$$

where a=-1^o and b=91200 (degree/nm). At d=$d_o\cong$1002.2 nm, θ_{out}becomes 90^o and hence the beam will be radiated normal to the antenna surface .

Its worthy to investigate the radiation pattern of the LWA when its fabricated with grating period slightly lower than d_o. let d=d_o+Δd which leads to θ_{out}=90^o+$\Delta\theta_{out}$. The fitting relation (Eqn. 10) yields

$$\Delta\theta_{out}\,(degree) = -\frac{b * \Delta d}{d_o(d_o + \Delta d)} \cong -\, b * \frac{\Delta d}{{d_o}^2} \quad for\ d_o \gg \Delta d \tag{11}$$

where b/d_o^2 =0.0908 (degree/nm). Eqn. 11 reveals that the deviation of the mail lobe direction from the normal direction decreases linearly with Δd when Δd/d<<1.

For example, Δd =$\pm$ 50 nm yields $\Delta\theta_{out}$= $\mp$ 4.65^o, these results are illustrated further in Figure 16 where the radiation pattern characteristics are plotted for Δd=0, +50 nm, and -50 nm, respectively.

Table5. List of the radiation parameters for different values of d chosen around the point of observation.

	Grating period (nm)					
Radiation parameter	**900**	**950**	**970**	**1000**	**1050**	**1100**
S_{11} (dB)	-14.15	-14.92	-14.27	-10.13	-21.59	-24.23
S_{21} (dB)	-22.22	-19.43	-18.29	-28.65	-22.32	-18.35
Radiation efficiency	0.88	0.88	0.87	0.67	0.82	0.85
Total efficiency	0.84	0.84	0.82	0.60	0.81	0.84
Directivity (dB)	21.93	22.53	19.77	20.31	18.98	14.30
Gain (dB)	19.21	19.71	17.10	13.50	15.57	12.2
Main lobe magnitude (dB)	22.04	22.58	22.76	20.29	21.99	21.21
Main lobe direction (degree)	101	95	93	90	86	82
Side lobe level (dB)	-8.2	-10.1	-9.3	-5.4	-8.8	-3.8
3dB angular width (degree)	3.6	3.1	3.0	2.7	2.9	3.4

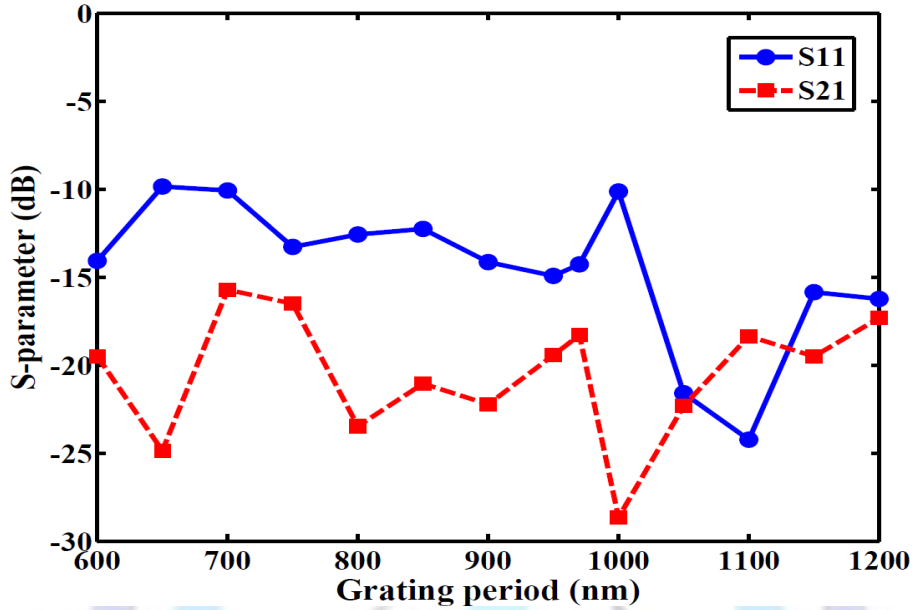

(a)

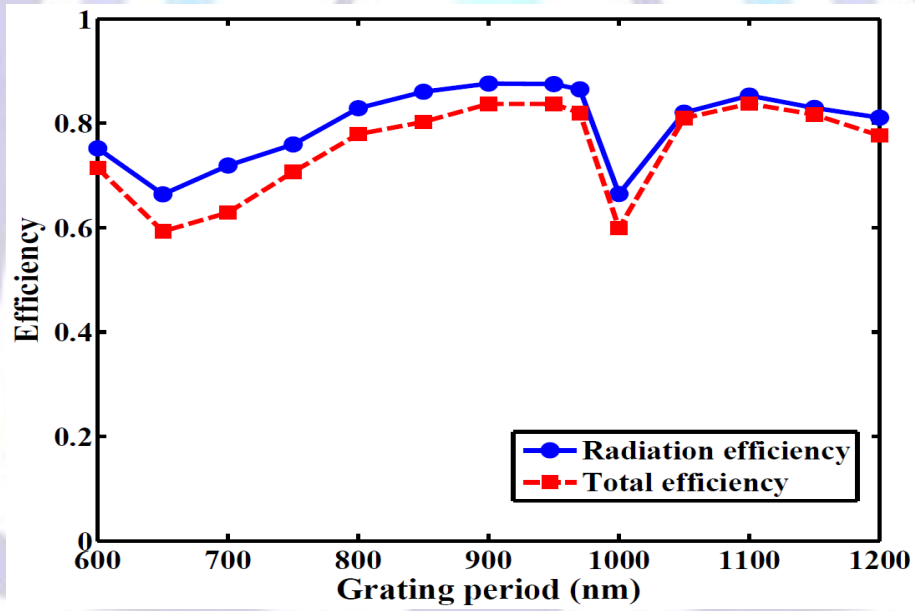

(b)

Fig 15: Variation of radiation parameters with perturbation period (a) S-parameter (b) efficiency (c) directivity (d) gain (e) main lobe magnitude (f) main lobe direction (g) side lobe level (h) 3 dB angular width.

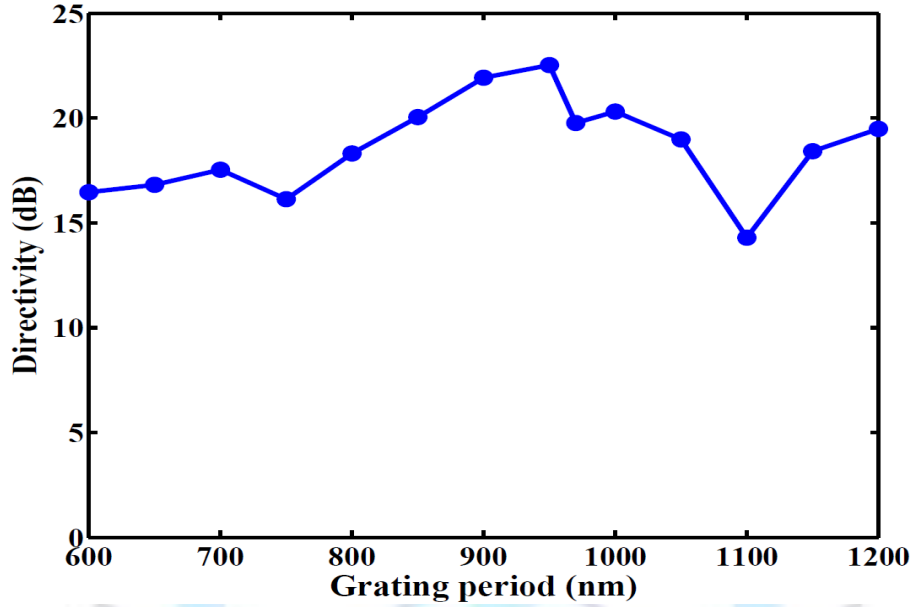

(c)

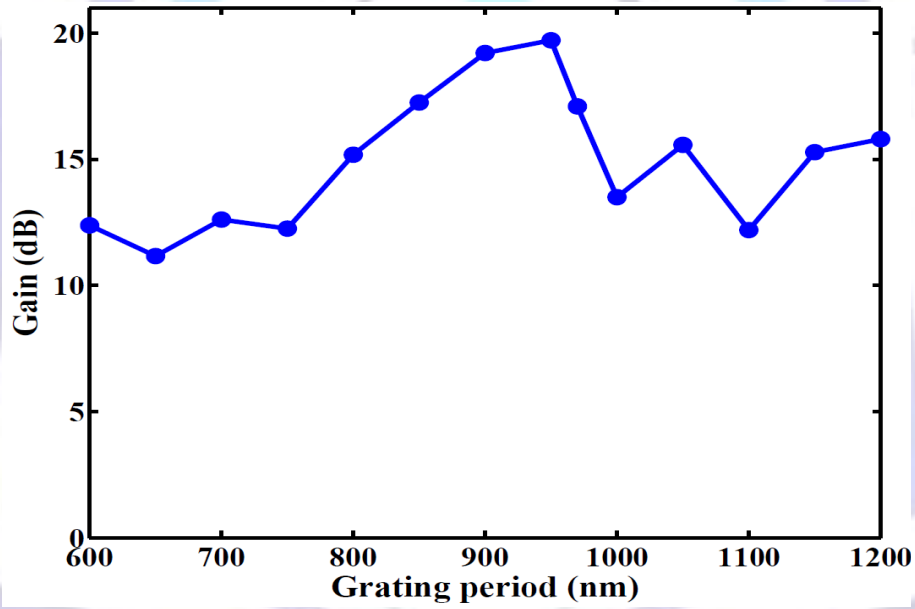

(d)

Fig 15: (Continued).

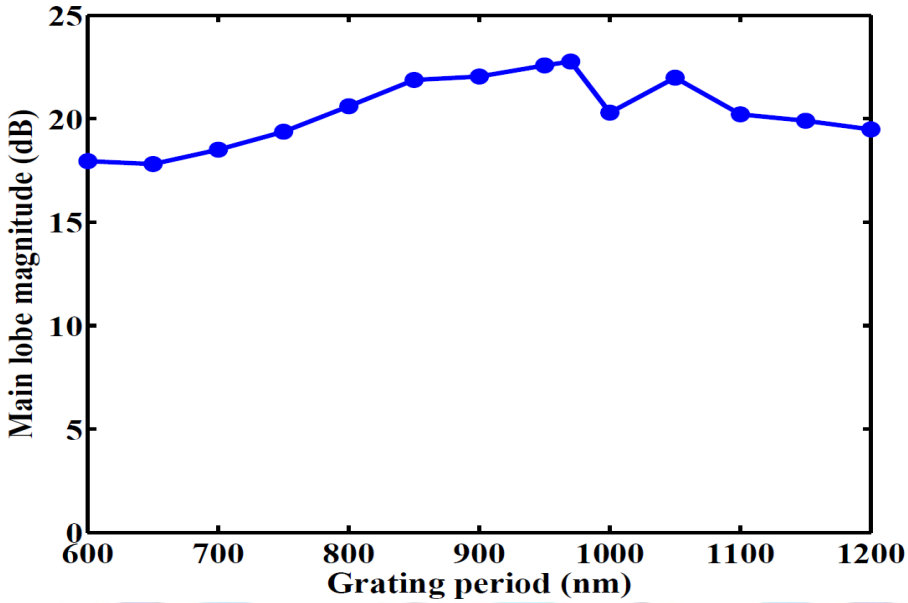

(e)

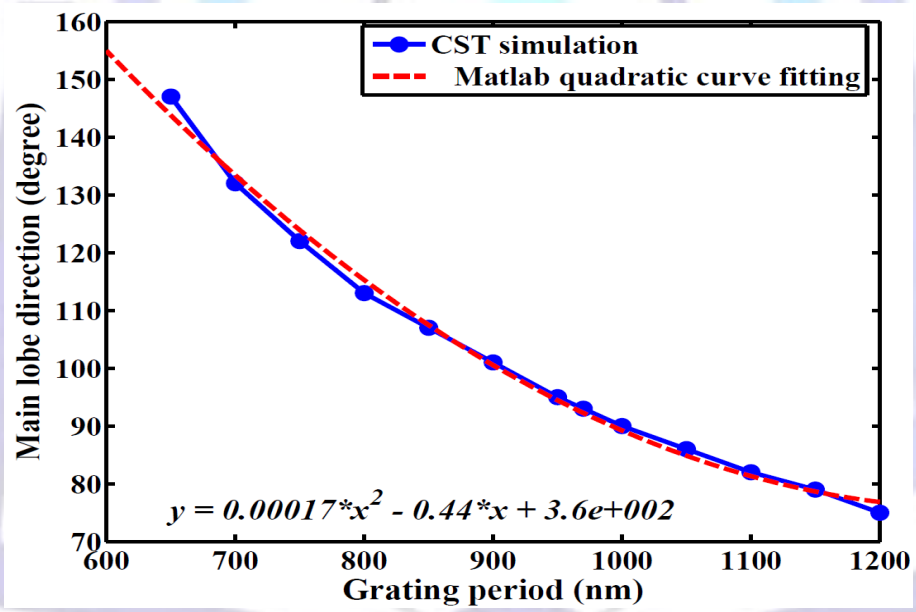

(f)

Fig 15: (Continued).

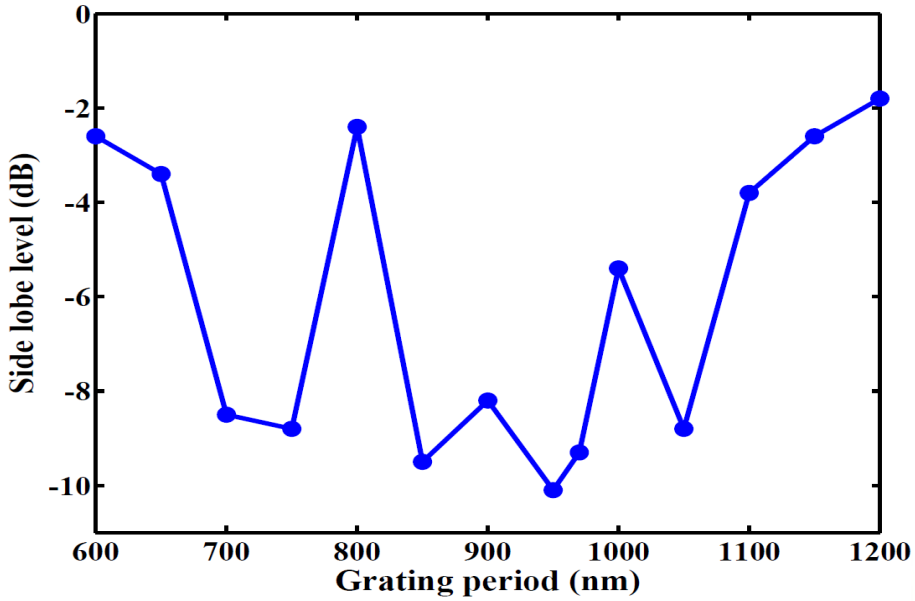

(g)

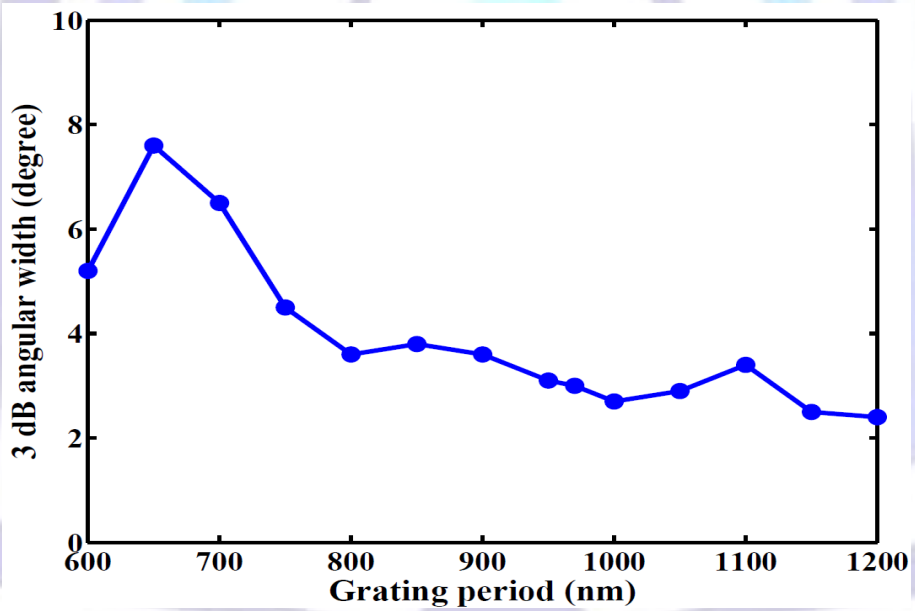

(h)

Fig 15: (Continued).

ISSN 2277-3061

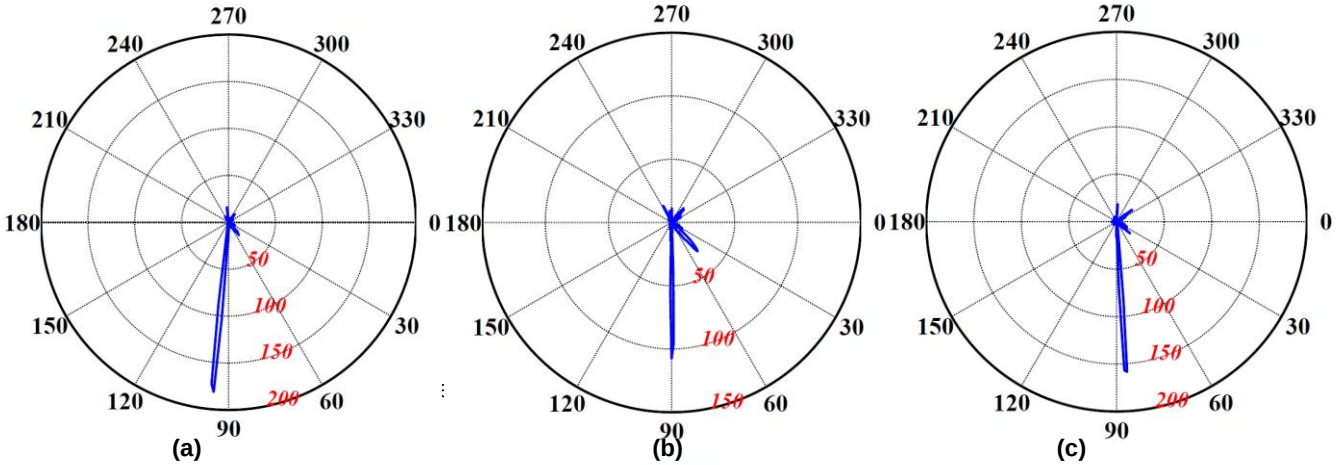

Fig 16: Variation of the main lobe direction with grating period when Δd/d<<1 (eqns. 1 and 2) (a)Δd=-50 nm (b)Δd=0 nm (c)Δd=+50 nm.

From 1400 nm to 1700 nm. The results are reported in Figures 17a-h for N=30 and summarized in Table 6 for specific wavelengths. The main findings from these Figures are

i. The antenna offers excellent characteristics at the reference wavelength (1550nm). At this wavelength, the total efficiency=0.820, radiation efficiency=0.861, gain=19.610 dB, and the 3dBangular beam width=3^{o}. Note also that the gain is maximum at this wavelength while the efficiencies are nearly maximum.

ii. Operating above or below the 1500 nm wavelength may degrade the antenna performance and this effect is more pronounced as λ approaches 1400 nm.

iii. The main lobe direction varies almost linearly with the wavelength. This is clear from Figure 17f where the dashed line is plotted using linear curve fitting method and has a slope of 0.071 degree/nm.
This result can be used to scan (steer) the radiated beam by turning the wavelength of the incident wave.

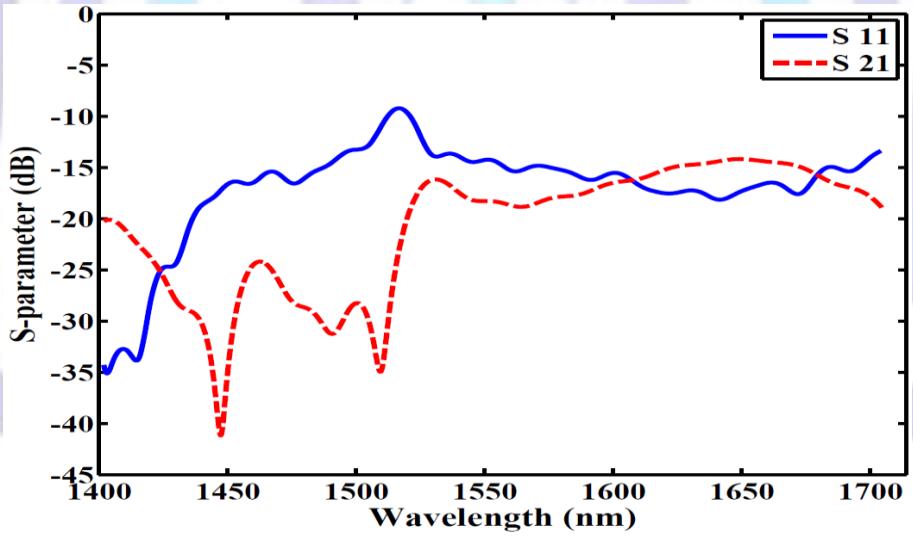

(a)

Fig 17: Variation of radiation parameters with wavelength (a) S-parameter (b) efficiency (c) directivity (d) gain (e) main lobe magnitude (f) main lobe direction (f) side lobe level (h) 3 dB angular width

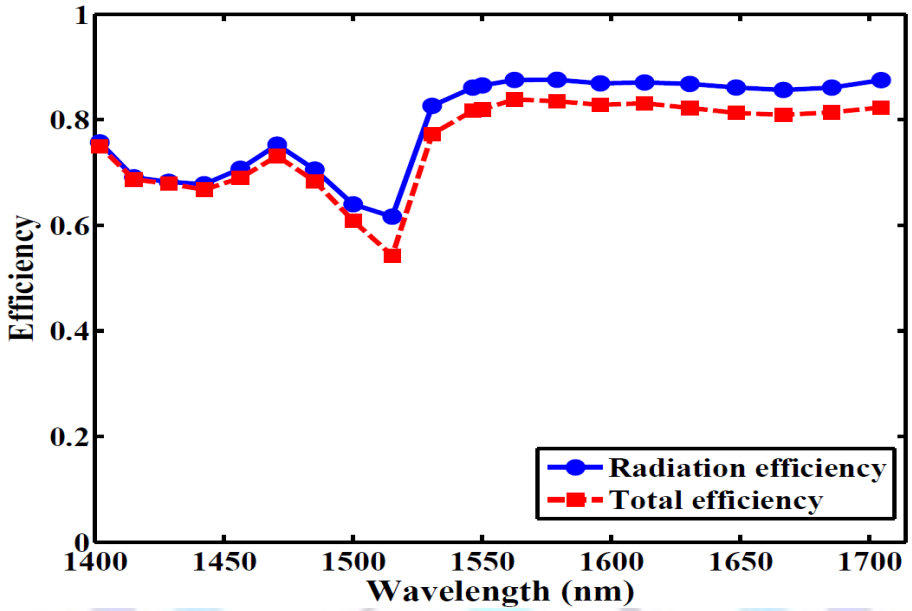

(b)

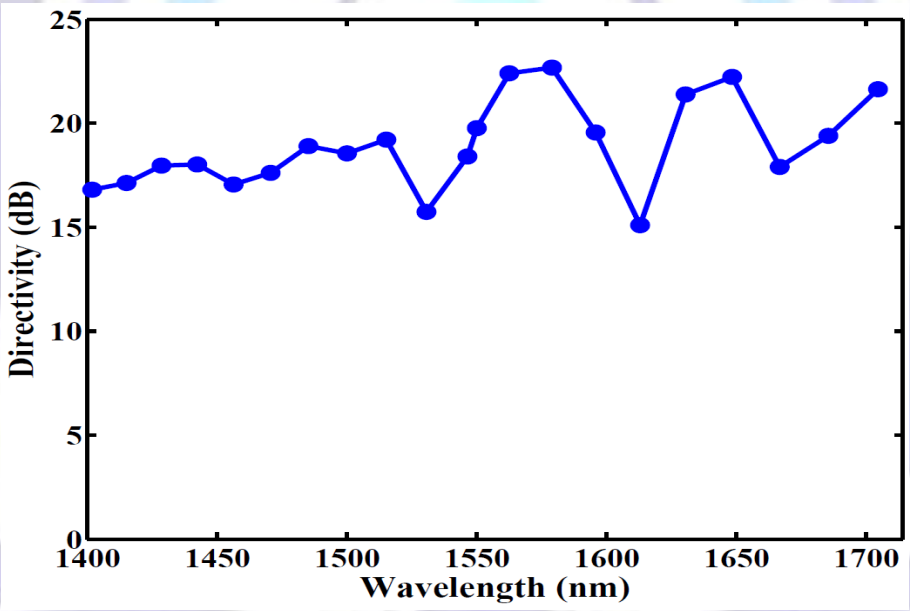

(c)

Fig 17: (Continued).

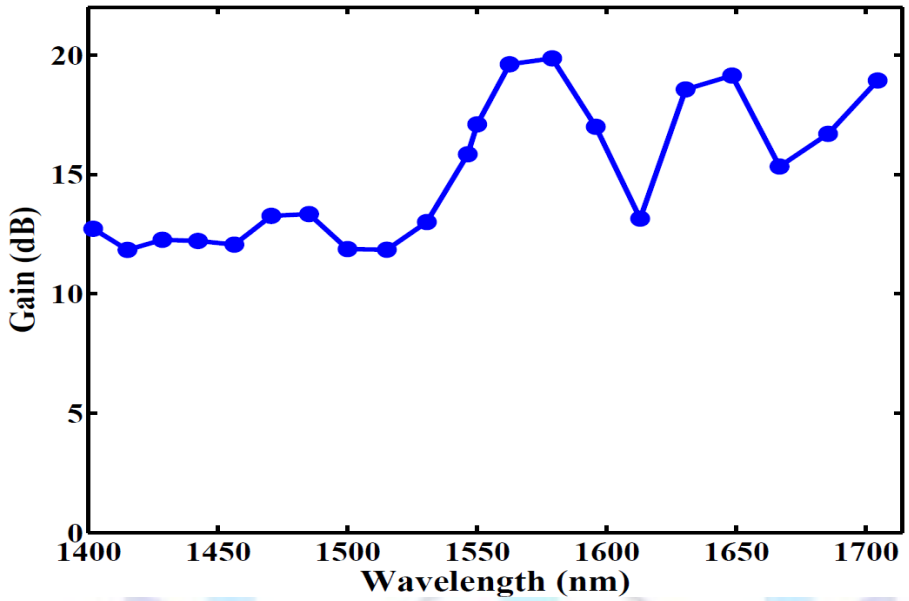

(d)

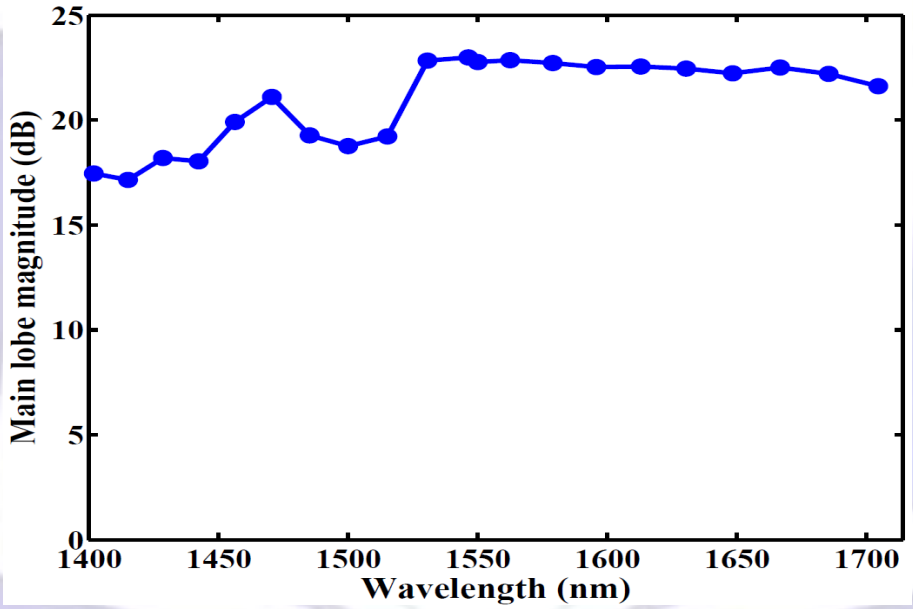

(e)

Fig 17: (Continued).

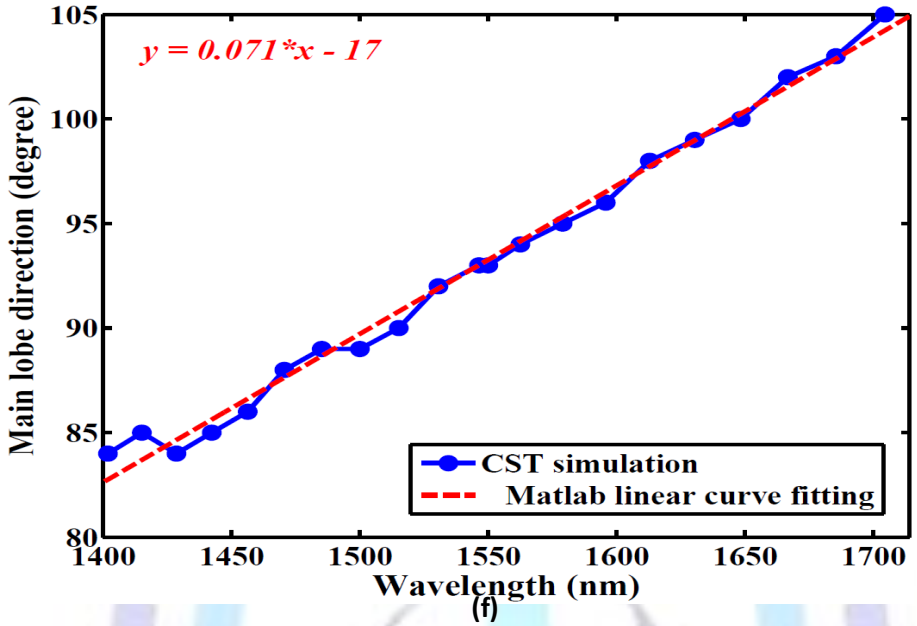

(f)

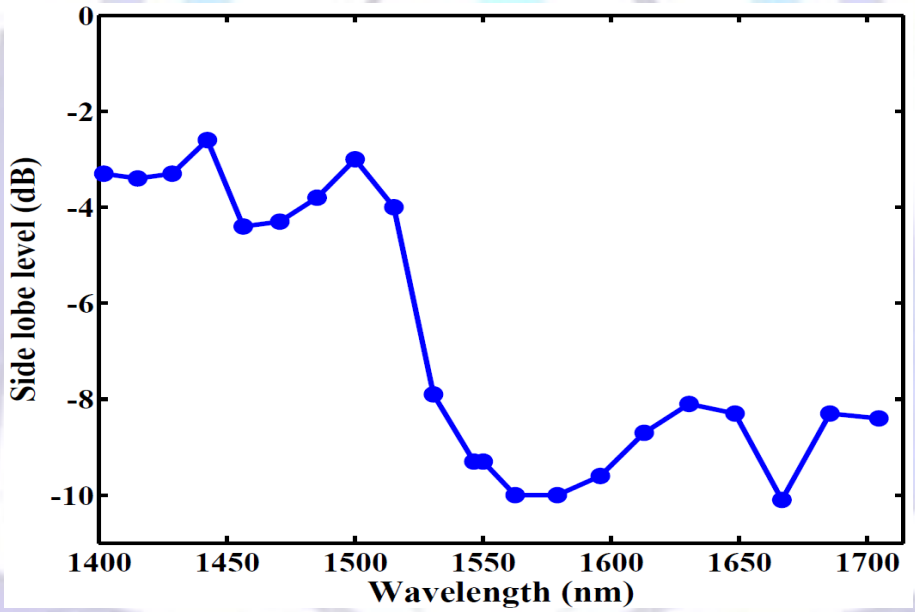

(g)

Fig 17: (Continued).

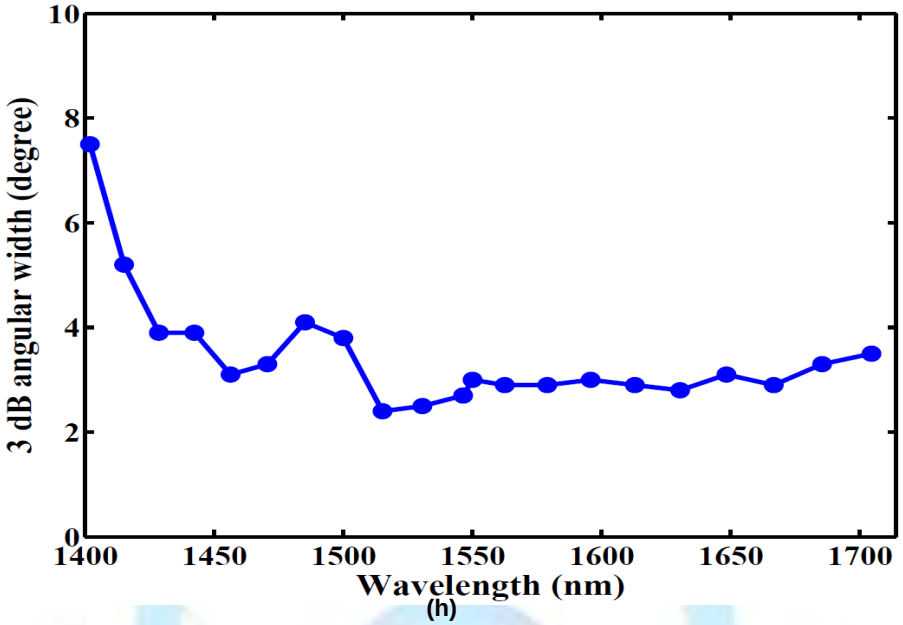

(h)

Fig 17: (Continued).

Table 6: Dependence of antenna radiation parameters on wavelength

Radiation parameters							
Wavelength (nm)	Radiation efficiency	Total efficiency	Directivity (dB)	Main lobe magnitude (dB)	Main lobe direction (degree)	3dB angular width (degree)	Side lobe level (dB)
1704.55	0.88	0.82	21.63	21.61	105	3.5	-8.4
1685.40	0.86	0.81	19.40	22.20	103	3.3	-8.3
1666.67	0.86	0.81	17.90	22.50	102	2.9	-10.1
1648.35	0.86	0.81	22.23	22.23	100	3.1	-8.3
1630.44	0.87	0.82	21.38	22.46	99	2.8	-8.1
1612.90	0.87	0.83	15.10	22.56	98	2.9	-8.7
1595.75	0.87	0.83	19.56	22.53	96	3.0	-9.6
1578.95	0.88	0.84	22.67	22.72	95	2.9	-10
1562.50	0.88	0.84	22.40	22.86	94	2.9	-10
1550.00	0.87	0.82	19.77	22.76	93	3.0	-9.3
1546.39	0.86	0.82	18.4.	22.99	93	2.7	-9.3
1530.61	0.83	0.77	15.74	22.83	92	2.5	-7.9
1515.15	0.62	0.54	19.21	19.22	90	2.4	-4.0
1500.00	0.64	0.61	18.55	18.76	89	3.8	-3.0
1485.15	0.71	0.68	18.90	19.27	89	4.1	-3.8
1470.59	0.75	0.73	17.60	21.11	88	3.3	-4.3
1456.31	0.71	0.69	17.06	19.91	86	3.1	-4.4
1442.31	0.68	0.67	18.02	18.03	85	3.9	-2.6
1428.57	0.68	0.68	17.97	18.20	84	3.9	-3.3
1415.09	0.69	0.69	17.13	17.15	85	5.2	-3.4
1401.87	0.76	0.75	16.81	17.46	84	7.5	-3.3

4. CONCLUSIONS

The effect of structure parameters on the performance of silicon-based optical leaky wave antenna has been investigated for 1550 nm operation. The main results drawn from this study are:

- Both radiation efficiency and total efficiency are increasing functions of N and this effect is more pronounced for N<10 where the efficiency increases almost linearly with the number of silicon perturbations.
- The radiation parameters vary slowly with bar width w in the region around w=483.75 nm. This region extends from 300nm to 550 nm for most radiation parameters.
- In the region 300-550 nm, the optimum value of w depends on the required radiation parameter to be optimized. For example maximum gain of 18.32 dB occurs when w=450 nm.
- The geometric dimensions of the silicon perturbations depend on the radiation parameter to be optimized.

5. REFERENCES

[1] A. Polemi and S. Maci, "A leaky-wave groove antenna at optical frequency", Journal of Applied Physics, PP. 074320-1- 074320-6, October 2012.

[2] A. Alù N. Engheta, "Wireless at the Nanoscale: Optical Interconnects using Matched Nanoantennas", The American Physical Society, PRL 104, PP. 213902-1- 213902-4, May 2010.

[3] C. Guclu, M. Veysi, O. Boyraz, and F. Capolino, "Optical Leaky-Wave Antenna Integrated in Ring Resonator", physics. Optics, Jan 2014.

[4] C. Guclu, S. Campione, O. Boyraz, and FCapolino, "Theory of a Directive Optical Leaky Wave Antenna Integrated into a Resonator and Enhancement of Radiation Control", Journal of Light wave Technology, VOL. 32, NO. 9, PP. 1741-1749, May 2014.

[5] C. M.-Segura, A. P. Feresidis, and G. Goussetis, "Bandwidth Enhancement of 2-D Leaky-Wave Antennas With Double-Layer Periodic Surfaces", IEEE Transactions on Antennas and Propagation, VOL. 62, NO. 2, PP. 586-593, February 2014.

[6] D. R. Jackson, P. Burghignoli, G. Lovat, F. Capolino, J. Chen, D. R. Wilton, and A. A. Oliner, "The Fundamental Physics of Directive Beaming at Microwave and Optical Frequencies and the Role of Leaky Waves", Proceedings of the IEEE | Vol. 99, No. 10, PP. 1780-1805, October 2011.

[7] D. Saxena, S. Mokkapati, C. Jagadish, "Semiconductor Nanolasers", IEEE Photonics Journal, Volume 4, Number 2, PP. 582-585, April 2012.

[8] D. R. Jackson, C. Caloz, and T. Itoh, "Leaky-Wave Antennas", Proceedings of the IEEE | Vol. 100, No. 7, PP. 2194-2206, July 2012.

[9] F. Xu, KeWu, *and* X. Zhang, "Periodic Leaky-Wave Antenna for Millimeter Wave Applications Based on Substrate Integrated Waveguide", IEEE Transactions on Antennas and Propagation, VOL. 58, NO. 2, PP. 340-347, February 2010.

[10] G. Lovat, P. Burghignoli, and D. R. Jackson, "Fundamental Properties and Optimization of Broadside Radiation From Uniform Leaky-Wave Antennas", IEEE Transactions on Antennas and Propagation, VOL. 54, NO. 5, PP. 1442-1452, May 2006.

[11] J. Sun, E. Timurdogan, A. Yaacobi, Z. Su, E. S. Hosseini, D. B. Cole, and M. R. Watts, "Large-Scale Silicon Photonic Circuits for Optical Phased Arrays", IEEE Journal of selected Topics in Quantum Electronics, VOL. 20, NO. 4, Conference, July/August 2014.

[12] J. Vaillancourt, N. Mojaverian, and X. Lu, "A Long wave Infrared Focal Plane Array Enhanced by Backside-Configured Plasmonic Structures", IEEE Photonics Technology Letters, VOL. 26, NO. 8, PP. 745-748, April 2014.

[13] J. Sun, E. Timurdogan, A. Yaacobi, Z. Su, E. S.Hosseini, D. B. Cole, and M. R. Watts, "Large-Scale Silicon Photonic Circuits for Optical Phased Arrays", IEEE Journal of Selected Topics in Quantum Electronics, VOL. 20, NO. 4, July/August 2014.

[14] K. Wei, Z. Zhang, Z. Feng, and M. F. Iskander, "Periodic Leaky-Wave Antenna Array With Horizontally Polarized Omni directional Pattern", IEEE Transactions on Antennas and Propagation, VOL. 60, NO. 7, July 2012.

[15] L. Yousefi and A. C. Foster, "Waveguide-fed optical hybrid plasmonic patch nano-antenna", Optics Express, Vol. 20, No. 16, PP. 18326-18635, July 2012.

[16] P. Bharadwaj, B. Deutsch, and L. Novotny, "Optical Antennas", Advances in Optics and Photonics, PP. 438-483, August2011.

[17] Q. Song, S. Campione, O. Boyraz, and F. Capolino, "Silicon-based optical leaky wave antenna with narrow beam radiation", Optics Express, Vol. 19, No. 9, PP. 8735-8749, Aril 2011.

[18] S. Otto, Z. Chen, A. Al-Bassam, A. Rennings, K. Solbach, and C. Caloz, "Circular Polarization of Periodic Leaky-Wave Antennas With Axial Asymmetry: Theoretical Proof and Experimental Demonstration", IEEE Transactions on Antennas and Propagation, VOL. 62, NO. 4, PP. 1817-1829, April 2014.

[19] S. K. Podilchak, L. Matekovits, A. P. Freundorfer, Y. M. M. Antar, and M. Orefice, “Controlled Leaky-Wave Radiation From a Planar Configuration of Width-Modulated Microstrip Lines IEEE Transactions on Antennas and Propagation, VOL. 61, NO. 10, PP. 4957-4972, October 2013”.

[20] S. Paulotto, P. Baccarelli, and D.R. Jackson, “A self-matched wide scanning U-stubmicrostrip periodic leaky-wave antenna”, Journal of Electromagnetic Waves and Applications, Vol. 28, No. 2, PP. 151–164, January 2014.

[21] S. Campione, C. Guclu, Q. Song, O. Boyraz, and F. Capolino, “An optical leaky wave antenna with Si perturbations inside a resonator for enhanced optical control of the radiation”, Optics Express, Vol. 20, No. 19, PP. 21305-21317, September 2012.

[22] Y. Wang, “Plasmonic Antennas and Arrays for Optical Imaging and Sensing Applications”, Department of Electrical and Computer Engineering University of Toronto, 2013.

[23] Y. Wang, A. S. Helmy, and G. V. Eleftheriades, “Ultra-wideband optical leaky-wave slot antennas”, Optics Express, Vol. 19, No. 13, PP. 12392-12401, June 2011.

[24] Z. Pan and J. Guo, “Enhanced optical absorption and electric field resonance in diabolo metal bar optical antennas”, Optics Express, Vol. 21, No. 26, PP. 32491-32500, December 2013.